TAMPEREEN TEKNILLINEN YLIOPISTO
TAMPERE UNIVERSITY OF TECHNOLOGY

NIKO ERKINTALO

A SOFTWARE TOOLBOX FOR NETWORK ANALYSIS OF MULTI-CHANNEL ELECTROENCEPHALOGRAM AND ITS APPLICATION TO MONITORING BRAIN FUNCTION IN THE INTENSIVE CARE UNIT

Master's thesis

Examiner: Professor Tarmo Lipping
Examiner and topic approved by the Council of The Faculty of Business and Built Environment 27.3.2017

ABSTRACT

NIKO ERKINTALO: A Software Toolbox for Network Analysis of Multichannel Electroencephalogram and its Application to Monitoring Brain Function in the Intensive Care Unit
Tampere University of Technology
Master of Science Thesis, 57 pages
May 2017
Master's Degree Programme in Management and Information Technology
Major: Software Engineering and Data Management
Examiner: Professor Tarmo Lipping

Keywords: EEG, electroencephalography, network analysis, connectome, data analysis, cross frequency coupling, biosignal, Matlab, analysis system

Use of electroencephalography (EEG) derived measures as predictors of outcome for various brain injuries and diseases has become an important field of study. There have been several studies where quantitative EEG (qEEG) features have been used to predict the outcome of treatment in brain injury patients or to detect seizures or other conditions difficult to assess clinically.

In this thesis, cross-frequency coupling and coherence based matrices are used as predictors of outcome in traumatic brain injury patients. For this analysis, a modular prototype of a software toolbox has been built using the Matlab environment.

Using the software toolbox, a dataset recorded in Turku University Hospital, including EEG data of 30 traumatic brain injury patients, has been considered. From these patients, 6 were selected for this preliminary study. Artifacts were removed using annotation files created by visually inspecting the data. From clean data, two types of connectivity matrices were calculated, one based on phase-amplitude coupling and the other based on magnitude squared coherence. Based on the known outcome of treatment in the ICU, the patients were divided into two groups. In total, 4910 matrices were included from the patients with positive outcome and 4103 matrices from the patients with negative outcome. Matrices in each group were obtained from several recordings of 3 patients.

Calculated values from matrices of each group were compared using the Mann-Whitney U-test. In the case of the Phase Amplitude Coupling (PAC) connectivity matrix, the frontal channels, especially Fp1, Fp2 and Fz, had higher values in patients with positive outcome. The coherence based connectivity matrix did not show as clear channel-wise correlations with the outcome, but the average coherence in the 13-35 Hz frequency band suggested higher values in patients with positive outcome in 76 % of the test cases.

These results cannot yet be considered clinically relevant, and further studies are needed to confirm the results.

TIIVISTELMÄ

NIKO ERKINTALO: Ohjelmistotyökalu verkostoanalyysin tekemiseksi monikanavaisesta aivosähkökäyrästä ja sen toteutus: aivotoiminnan monitorointi tehoosastolla
Tampereen teknillinen yliopisto
Diplomityö, 57 sivua
Toukokuu 2017
Johtamisen ja tietotekniikan diplomi-insinöörin tutkinto-ohjelma
Pääaine: Ohjelmistotuotanto ja tiedonhallinta
Tarkastaja: professori Tarmo Lipping

Avainsanat: EEG, aivosähkökäyrä, verkostoanalyysi, konnektomi, data-analyysi, taajuuskaistojen kytkeytyneisyys, biologiset signaalit, Matlab, analyysi-järjestelmä

Aivosähkökäyrästä johdettujen mittareiden käyttäminen potilaan lopputuleman ennustamisessa aivovauroiden sekä aivoperäisten sairauksien kohdalla on muodostunut tärkeäksi tutkimusalaksi. Aivosähkökäyrästä johdettuja määrällisiä piirteitä (qEEG) on käytetty lukuisissa tutkimuksissa aivovauriopotilaan lopputuleman ennustamisessa sekä kohtausten havainnoinnissa ja muissa kliinisesti vaikeasti havaittavissa tilanteissa.

Tässä työssä käytetään taajuuskaistojen välisen kytkeytyneisyyden (CFC, Cross Frequency Coupling) ja koherenssin pohjalta laskettuja matriiseja ennustamaan aivovauriopotilaan hoidon lopputulemaa. Tätä analyysiä varten suunniteltiin ja toteutettiin ohjelmistotyökalun modulaarinen prototyyppi Matlab-ympäristössä.

Turun yliopistollisen keskussairaalan taltioimaa, 30 aivovauriopotilaan kattavaa materiaalia tutkittiin kehitetyn työkalun avulla. Kuusi potilasta valittiin näiden 30:n joukosta analysoitavaksi tämän työn puitteissa. Valittujen potilaiden aivosähkökäyristä poistettiin artefaktat visuaalisen tarkastelun perusteella luotujen annotaatio-tiedostojen avulla. Puhtaasta datasta laskettiin konnektiivi-matriisit käyttäen vaihe-amplitudi kytkeytyneisyyttä sekä koherenssia. Tehohoidon lopputuleman perusteella potilaat jaettiin positiiviseen ja negatiiviiseen ryhmään. Positiivisen ryhmän potilaiden osalta tutkittavia matriiseja oli 4910 ja negatiivisen ryhmän kohdalla 4103. Kummankin ryhmän matriisit muodostettiin kolmen ryhmään kuuluvan potilaan taltioinneista.

Ryhmien matriiseja verrattiin Mann-Whitneyn U-testillä. Vaihe-amplitudi kytkeytyneisyyden kohdalla positiivisen lopputuleman ryhmän EEG:n etukanavien, (eritoten Fp1, Fp2 ja Fz) havaittiin omaavan suurempia arvoja kuin negatiivisen lopputuleman ryhmän. Koherenssin kohdalla yhtä suuria kanavakohtaisia korrelaatioita ei ollut havaittavissa, mutta keskimääräinen koherenssi 13-35 Hz taajuuskaistalla oli suurempi positiivisen ryhmän kohdalla 76 %:ssa testitapauksista.

Tuloksia ei voida pitää vielä kliinisesti merkityksellisinä, mutta saavutetut tulokset osoittavat, että tutkimuksen laajentaminen kattamaan eri konnektiivisuusmittareita ja koko käytettävän aineiston on perusteltua.

PREFACE

This thesis was done for the department of Pori at the Tampere University of Technology (TUT). The project was introduced to me by Professor Tarmo Lipping, who I wish to thank for providing the subject and especially for instructing, helping and teaching me with great patience during this thesis and prior to it. I also wish to thank the whole faculty of the TUT at Pori for providing a positive atmosphere and flexible means to study while working.

When I started my studies, I could have never thought my thesis to deal with subjects such as EEG or network analysis, but I am extremely happy that this is the case. This thesis has required a lot of new theories and concepts to be learnt and has introduced completely new fields of study to me. Although this has required a lot of studying, work and especially time, I feel it has been a great privilege.

In Pori, Finland on May 12, 2017

Niko Erkintalo

TABLE OF CONTENTS

LIST OF FIGURES

LIST OF ABBREVIATIONS

AUC	Area Under Curve
BNA	Brain Network Activation
CCEEG	Critical Care EEG
cEEG	Continuous EEG
CFC	Cross-Frequency Coupling
CT	Computed tomography
DFT	Discrete Fourier Transform
ECG	Electrocardiography
EDF	European Data Format
EDFbrowser	An open source software for EDF file inspection
EEG	Electroencephalography
EMG	Electromyography
EOG	Electrooculography
EPSP	Excitatory Postsynaptic Potential
FCG	Functional Connectivity Graph
FFT	Fast Fourier Transform
fMRI	Functional Magnetic Resonance Imaging
GCS	Glasgow Coma Scale
GOS	Glasgow Outcome Scale
GOSE	Glasgow Outcome Scale Extended
GPD	Generalized Periodic Discharge
GRDA	Generalized Rhythmic Delta Activity
GSW	Generalized Spike-and-Wave
ICA	Independent Component Analysis
IPSP	Inhibitory Postsynaptic Potential
LPD	Lateralized Periodic Discharge
LRDA	Lateralized Rhythmic Delta Activity
Matlab	Software of Matrix Laboratories
MCI	Mild Cognitive Impairment
MEG	Magnetoencephalography
MI	Mutual Information
MRI	Magnetic Resonance Imaging
MTBI	Mild Traumatic Brain Injury
NaN	Not a Number
PAC	Phase-Amplitude Coupling
PD	Periodic Discharge
PLV	Phase Locking Value
ROC	Receiver Operating Characteristic
SEF	Spectral Edge Frequency
TBI	Traumatic Brain Injury
TSA	Tensor Subspace Analysis
wICA	Wavelet –Independent Component Analysis
XML	Extensible Markup Language
XSD	XML Schema Definition

1. INTRODUCTION

The human brain has always been a matter of great interest in the world of science. A new discipline of electrical brain study was initially born in the 18th century, when Luigi Galvani discovered that electricity played a crucial part in the nervous system of a frog. Several centuries later, various mechanisms behind the function of the human brain are still unknown. Although technology has advanced a lot since the 18th century and many ways to study the brain have been invented, EEG remains the only method of measuring the actual electrical activity of brain function. EEG enables unintrusive study of the brain function portably with lightweight measuring devices and with good temporal accuracy and it can be used for constant real-time monitoring. In addition, EEG is highly cost-effective when compared to other techniques of brain study such as blood oxygenation based functional Magnetic Resonance Imaging (fMRI) or Magnetoencephalography (MEG) that measures the magnetic fields produced by brain electric activity.

EEG has been used as a tool of brain function monitoring since the beginning of the 20th century and it has proven itself as a cost-effective method for studying the brain's electrical functions. It can be considered the only method that, for example, Intensive Care Units (ICU) can use rapidly for multiple patients either for continuous EEG monitoring (cEEG) or for routine EEG measurements. This has led to increasing number of applications that use the indicators derived from the EEG as predictors for different conditions and outcomes. Among other areas, EEG has been extensively used and studied in the fields of epilepsy, general anesthesia, brain trauma, sleep as well as other similar conditions that affect the nervous system and the brain. There are various known characteristics and measures that can be used to evaluate the human brain using the EEG. A promising characteristic, having gained a lot of popularity recently, is the coupling effect between different brain regions and frequency ranges. Results from several studies suggest that different techniques for the assessment of coupling can be used to form indicators of the brain's network-like functionality. Using this information, a broad range of methodologies of network and graph studies have been successfully used to describe the connections between the brain regions.

The main focus of this thesis is on building a toolbox for studying the synchronicity measures between brain regions (EEG channels) from which brain network measures can be calculated. These network measures can be used to describe the connectivity, clustering and small-world phenomenon of the brain. Two following chapters (2 and 3) introduce the theoretical framework the toolbox is based on. The toolbox itself is presented in chapter 4; chapter 5 presents the results of applying the toolbox to the EEG data recorded from brain trauma patients while chapter 6 concludes the thesis.

2. ELECTROENCEPHALOGRAM

The discipline of electrophysiology was born when Luigi Galvani accidentally noticed the effects of static electricity on a dead frog's behavior. Therefore, he is considered as the pioneer of the electrophysiology (Empson 1986). The electroencephalography or EEG as a tool of measurement was discovered in 1875 when Richard Caton found that the electric currents were involved also in the brains of animals. Almost 50 years later in 1924 Hans Berger succeeded in measuring weak electric currents externally, from the human scalp (Teplan 2002). These measurements along with his other findings were published in his paper "Über das Elektrenkephalogramm des Menschen (On the EEG in humans)" (Berger 1929; Haas 2003).

Berger was the first to measure brain waves, but he was not fully aware of the physiological basis of their existence. Berger's theory led to an assumption that the brain was producing energy and transforming it to heat, electricity and 'physical energy'. The physical energy was the actual phenomenon he was trying to discover and the discovery of the brain waves was a side product of his studies. (Andersen & Andersson 1968)

Figure 1 shows one of the earliest recordings of human brain waves (the top signal). Only 5 years after the first recordings, due to fast development of the measurement devices (galvanometers) and Berger's focus on the brain study, the quality of his recordings were improved and he had already discovered different waveforms and named some, such as the alpha wave (Figure 2).

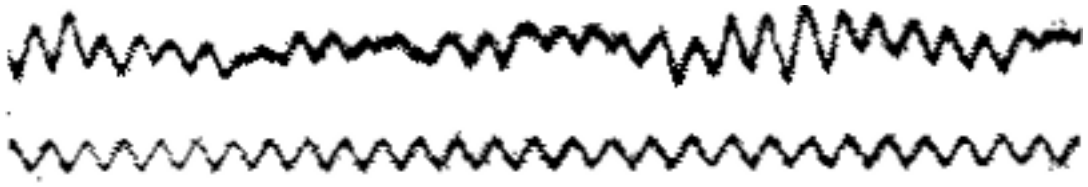

Figure 1. *The first recording of human brain waves (top signal) by Berger in 1924. The bottom signal is a 10 Hz reference.*

Figure 2. *Two recordings of EEG by Berger in 1928-1929, which show bursts of alpha waves (lower). Adapted from* (Barwick 1971; Millett 2001)

2.1 Origin and measurement of Electroencephalogram

EEG is a method of graphically representing changes in low voltage electrical activity of the brain. EEG can be measured either externally (unintrusively) from the scalp or the electrodes can be installed at the surface of the cerebral cortex or within the substance of the brain. In this thesis, if not otherwise stated, EEG refers to externally measured EEG.

When measuring the EEG we are mostly measuring extracellular summation of post-synaptic potentials of neural cells (neurons). This includes excitatory (EPSP) and inhibitory (IPSP) postsynaptic potentials, depending on if the cell membrane of the postsynaptic cell is depolarized (thus increasing the likelihood of the cell to fire) or hyperpolarized (thus decreasing the likelihood of the cell to fire), respectively (Olejniczak 2006)(Figure 3). When measuring the EEG from the scalp, there is no method to measure the electrical field of a single neuron. Instead, a large group of neurons can together create an electric field that is large enough to penetrate the tissue between the brain and the scalp and strong enough to be measured (Figure 4).

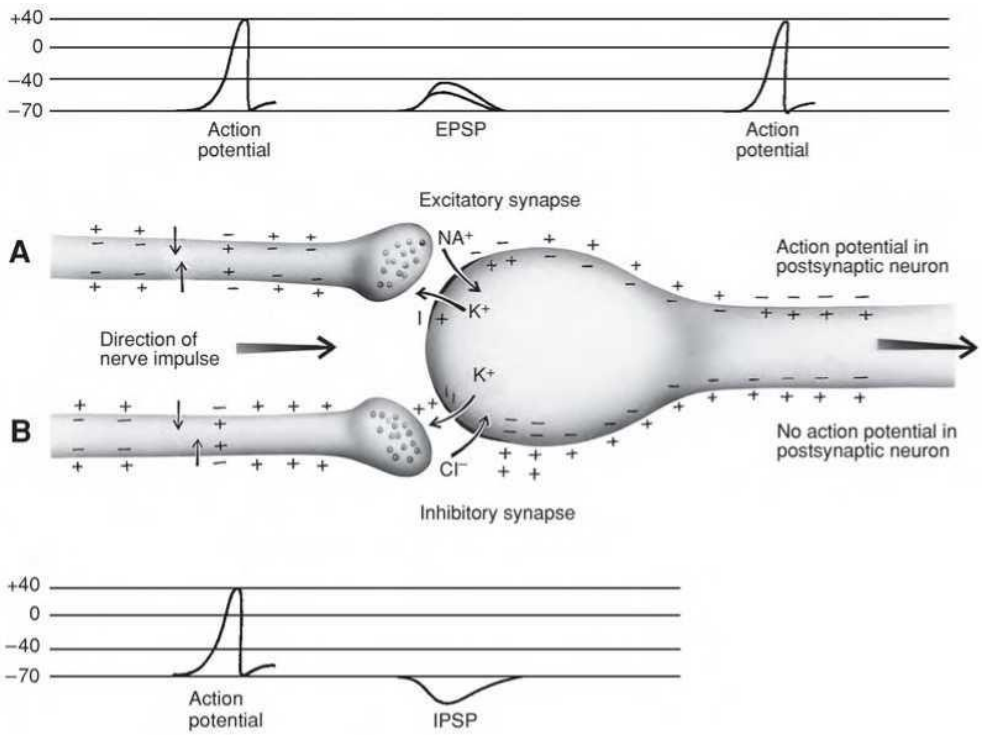

Figure 3. *Generation of EPSP and IPSP currents.* [1]

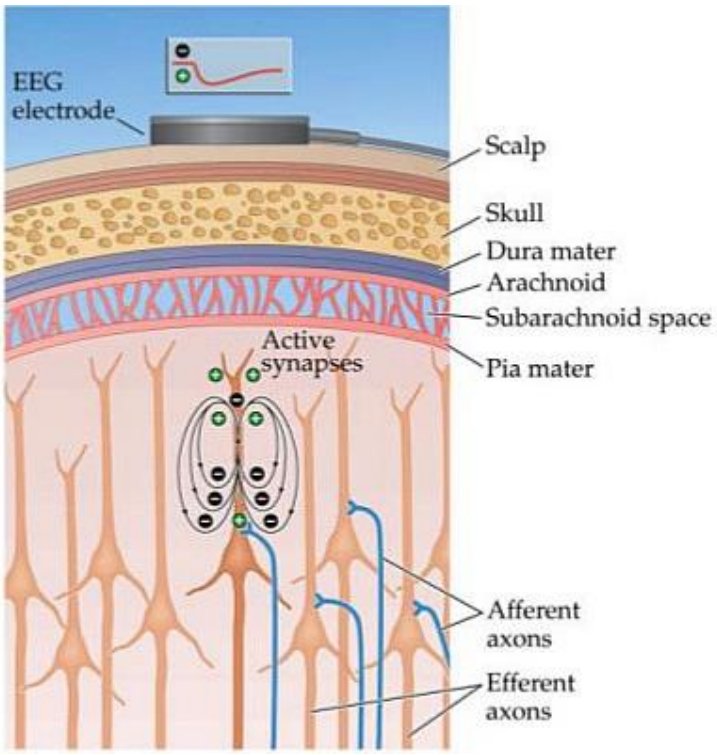

Figure 4. *Generation of measurable voltage differences (EEG).* [2]

[1] http://aibolita.com/nervous-diseases/47834-action-potentials.html
[2] https://www.slideshare.net/kj_jantzen/biophysical-basis-of-eeg

The summation of these postsynaptic potentials is generated from local current flows or local field potentials, which arise when the neurons are activated. The current flow is actually the flow of positive charge formed as the net flow of positive and negative ions, which cause a change in the voltage over the cell membrane.

When measuring the EEG, electrodes are placed at different locations of the scalp. The most commonly used system for electrode positioning is the 10-20 system (Figure 5). It has been used broadly since it was introduced in 1949 by Dr. Herbert H. Jasper. The 10-20 system gets its name from the percentual measurements of the subject's skull that dictate the positions of the electrodes (Klem et al. 1999).

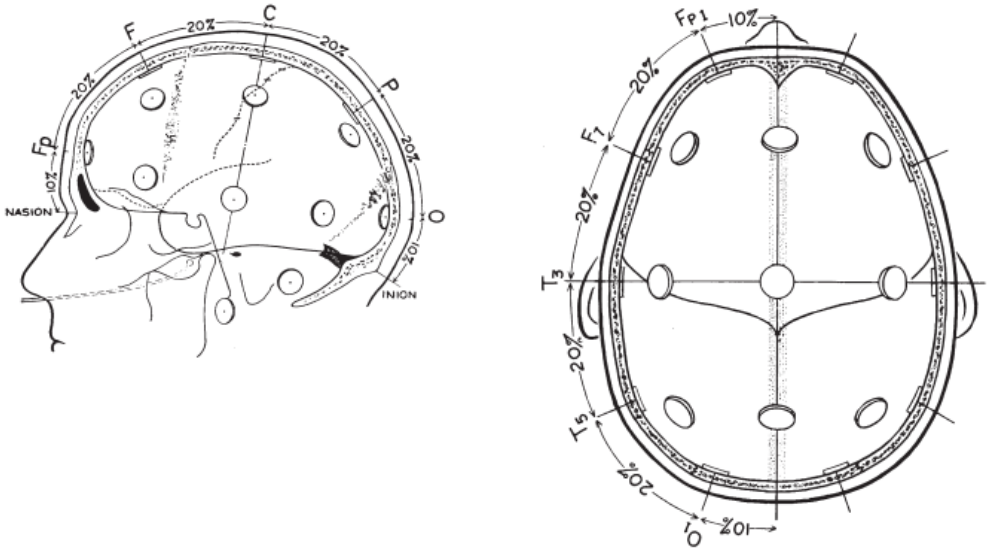

Figure 5. *10–20 System electrode placement* (Teplan 2002).

The electrodes are named using a naming convention based on their position on the skull. The naming of each electrode contains a letter or letters and a number. The letter(s) indicate the lobe and the number identifies the hemisphere location. In 10-20 system, the cortex is divided into 6 areas: Frontopolar (Fp), Frontal (F), Central (C), Temporal (T), Parietal (P) and Occipital (O) (Figure 5). Electrodes are numbered so that the electrodes on the left side of the skull are odd-numbered and the electrodes on the right side are even-numbered. The electrodes on the left hemisphere of the skull are, for example, Fp1, F7, F3, T3, C3, T5, P3 and O1. On the right hemisphere there are the counterparties Fp2, F8, F4, T4, C4, T6, P4 and O2. The midline electrodes Fz, Cz and Pz are located on the central line between nasion and inion (Figure 6).

The system can be extended by adding more electrodes between the existing ones. For example, F5 electrode could be added between F7 and F3 and its counterpart F4 between F2 and F6.

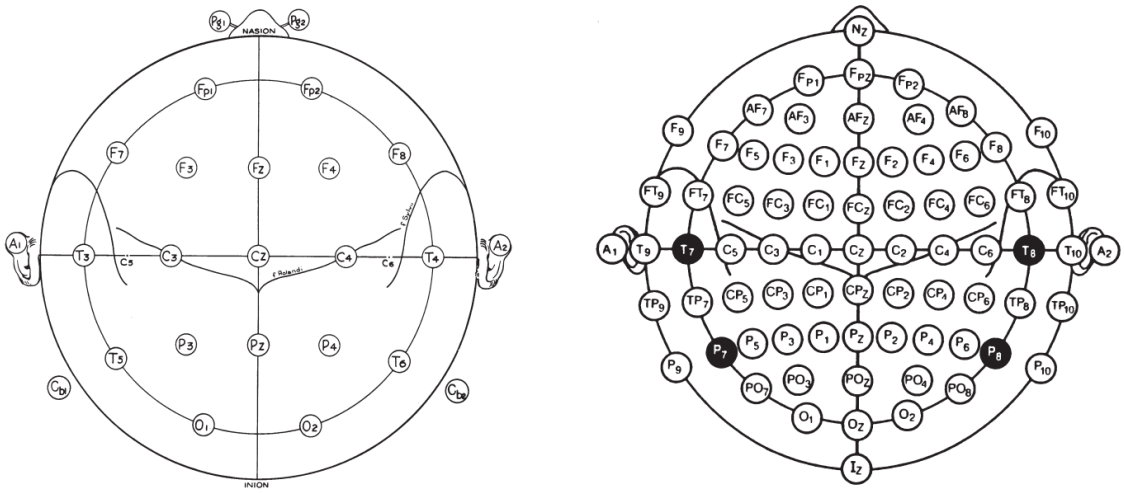

Figure 6. *The positions and naming of electrodes in the 10-20 system. The electrode placement of the standard 10-20 system on the left and extended on the right* (Teplan 2002).

2.2 Interpretation and description of the EEG

Digital EEG recording is simply a set of numeric time series data. There are two methods of gathering the data: unipolar and bipolar. In the case of unipolar measurement, each sample in the recording represents the voltage between the particular electrode and the reference electrode at the time of the measurement. In bipolar measurement, the potential differences are measured between electrode pairs. The numerical values of the EEG alone do not tell much about the data or the patient, but the series of measurements can be used as a basis for numerous methods of calculation and analysis. A common approach to examine the EEG is by simply plotting the time series data and allowing an expert to study it visually either in real time or from a recorded dataset. This method is frequently used to find obvious abnormalities that would explain certain symptoms in a patient in real time monitoring.

When looking for abnormalities, the medical background and condition of the patient must be taken into consideration. There are multiple factors that affect what can be considered as normal when interpreting the EEG, such as age and sex (Matsuura et al. 1985), medication (Centorrino et al. 2002), illnesses (Jeong 2004) etc. When the analysis of a recording or monitoring is performed by a machine, artifact detection is one of the key aspects to be considered. Artifact detection must work in a manner that no viable information is lost and on the other hand not too many alarms are falsely raised due to artifacts. Commonly the automatic interpreters are built as expert systems to assess or locate certain conditions. These systems can be used to detect various anomalies in the EEG such as spikes and sharp waves related to epilepsy (Davey et al. 1989), general abnormalities (Si et al. 1998) or alertness and drowsiness (Vuckovic et al. 2002), for example. When the

studied condition is narrow enough, artifact detection and other preprocessing can be customized to the needs of the system at hand for better results.

There are various areas of application, where EEG can be used to either predict or to monitor and alert of certain abnormalities or patterns. The final decisions are, however, made by medical experts, commonly neurologists or neurophysiologists.

2.2.1 Normal waveforms

The most common classification of the EEG waveforms uses frequency as the main parameter of separating individual rhythms. These rhythms have been categorized into five main groups according to the frequency band (Table 1).

Table 1. *EEG rhythms and corresponding state of awareness in healthy subjects*

Name	Frequency range	Awareness/asleep characteristics
delta	< 4 Hz	Asleep
theta	4 - 7 Hz	Awake and emotional or at deep sleep
alpha	8 - 13 Hz	Awake and relaxed
beta	13 - 30 Hz	Awake and alert
gamma	> 30 Hz	Learning or REM-sleep, no clear consensus

The frequency ranges are not standardized and in different contexts they might differ remarkably. For example, the gamma band might start from as low as 20 Hz (Miltner et al. 1999) or as high as 40 Hz (Lachaux et al. 2005) depending on the study. In a heathy subject, each rhythm relates to different aspect of awareness or state of alert, although, people of different age and sex have minor differences on what can be considered as normal in different stages of sleep and/or awareness. Figure 7 shows exemplary characteristics of each waveform.

2.2.2 EEG in frequency domain

In the EEG, the measured voltage differences are represented as a function of time. To study the different frequency bands, the signal must be converted into frequency domain, where the amplitude or power in the EEG is represented as a function of frequency instead of time.

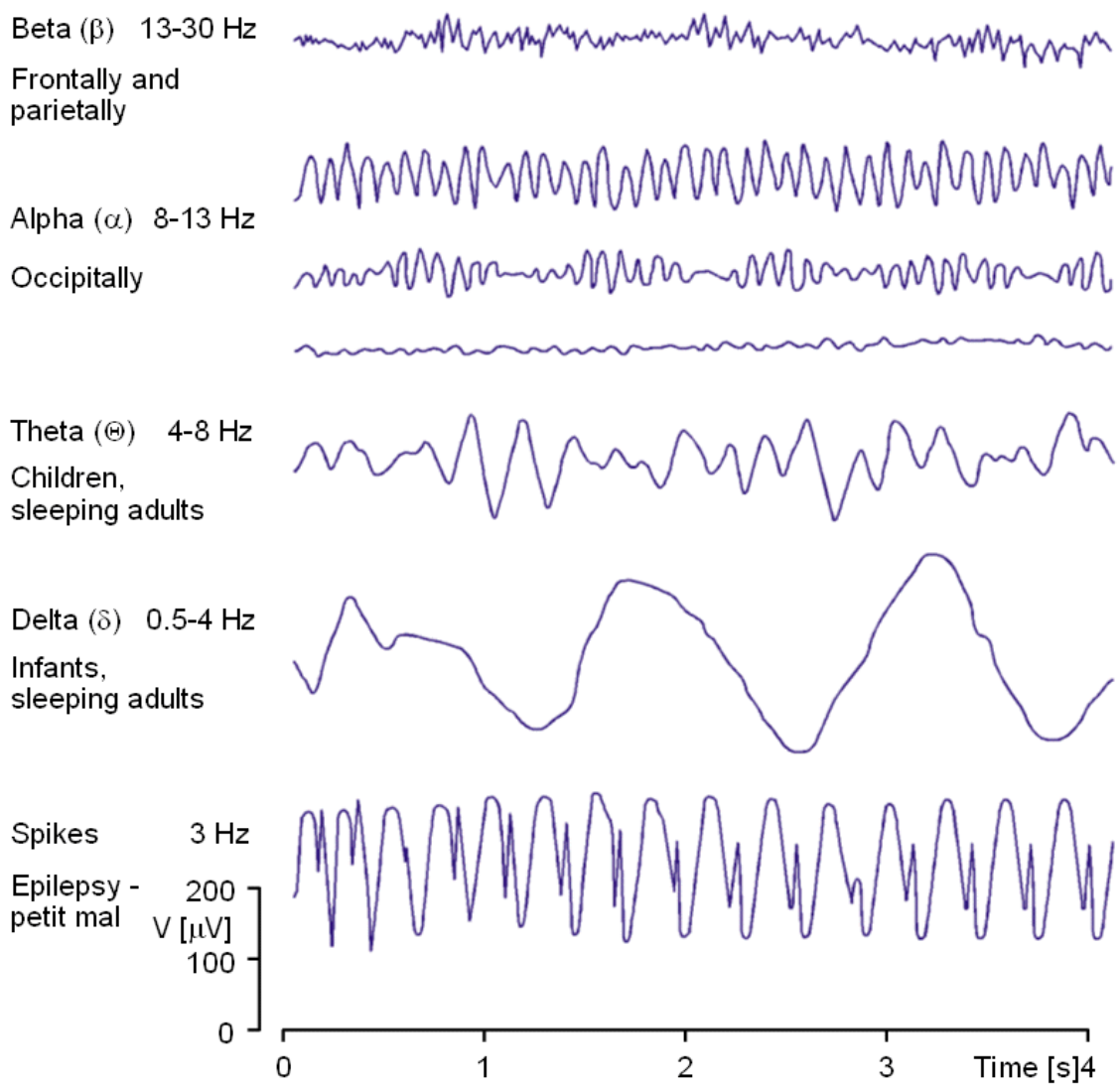

Figure 7. *Some examples of EEG waves* (Malmivuo & Plonsey 1995).

Frequency domain transform

The transformation method commonly used to transform the EEG from time domain to frequency domain is the Fourier transform. The Fourier transform reverse engineers the given signal to complex exponentials of different frequency which, when summed together, form the original signal. The Fourier transform is sometimes referred to as the forward transform, meaning, that the transformation is done towards the frequency domain. The counterpart, the inverse transform, reverses the forward transform and returns the original signal from its frequency domain representation.

The basic form of the Fourier transform is for transforming continuous signals. Real-life data such as EEG is nowadays commonly recorded using digital devices and, in that sense, is not continuous. This kind of discrete-time data is transformed using a discrete

version of the Fourier transform, the Discrete Fourier Transform (DFT), which can be expressed as:

$$X_k = \sum_{n=0}^{N-1} x_n \, e^{-2\pi i n k / N} \, ,$$

where N is the number of samples in a signal segment and k is the frequency of the particular value in the transform domain. As the continuous Fourier transform, DFT is also reversible and the inverse DFT is expressed as:

$$x_n = \frac{1}{N} \sum_{n=0}^{N-1} X_k \, e^{2\pi i n k / N} \, .$$

There are other valid techniques to perform the domain transformation. One of these techniques is the wavelet transform. The wavelet transform offers a different approach when compared to the Fourier transform. Where Fourier transform uses summation of (complex) sine waves, the wavelet transform uses a number of time-limited wavelets to deconstruct the signal. Due to the limited time base of the wavelets, the time resolution is preserved also in the frequency (or wavelet) domain. In a dimensional comparison, the wavelet transform can be considered 2D and the Fourier transform, lacking the time dimension, 1D. Despite their differences, the wavelet transform can be considered as an extension to Fourier type analysis (Chien Yong et al. 2013). It has been argued that EEG analysis would benefit from the usage of the wavelet transform instead of the commonly used Fast Fourier Transform (FFT) (Akin 2002; Yamaguchi 2003; Chien Yong et al. 2013).

Power spectral density

Power spectral density (PSD) can be used to indicate power as a function of frequency and therefore to observe the distribution of the signal power over frequencies. PSD can be used to monitor the awareness of the patient based on the existence and relative power of different rhythms. PSD is defined as the Fourier transform of the autocorrelation function (Mack 2011).

As the PSD relies on the theory of random signals, it can be interpreted as an estimate of the distribution of signal power in the frequency domain. Different kinds of methods exist for estimating the PSD. These methods can be roughly categorized as parametric and nonparametric methods. Parametric methods such as autoregressive modelling are based on a model built of the original signal. Nonparametric methods such as the Welch method, for example, use the DFT directly, therefore there is no need for modeling or parametrization of the signal. The window type and size define the resolution in which the PSD is estimated. A comparison of four PSD calculations using two methods with two different parameter sets each applied to the same EEG signal segment is shown in Figure 8. Frequencies from 0 to 35 Hz are estimated from a single channel (C4) of EEG data. Sampling

frequency of the data used in the estimation is 200 Hz and the length is 245000 samples. The top panels show the results of the estimation calculated using the Welch's method, with different sized (hamming) windows. The left part of the figure is estimated using a window of size 100 samples and the right using a 2000 samples long window. The bottom figures are calculated using a parametric method (Burg Estimate) with model orders of 4 (left) and 16 (right). The smoothness and the estimation accuracy of the PSD depends largely on the parameters used in the calculation.

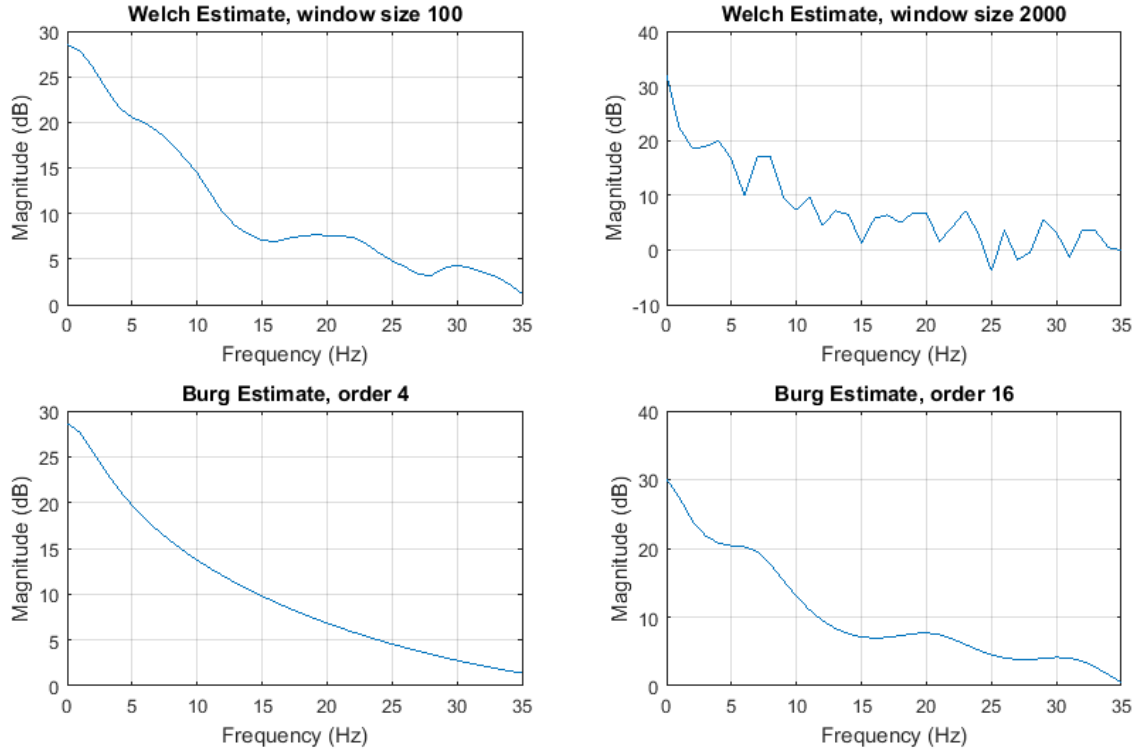

Figure 8. *Four PSD estimates calculated from a single channel of an EEG signal segment. Data estimated consists of 245000 samples and is recorded using 200 Hz sampling frequency.*

Frequency domain parameters

The properties of the EEG signal are often quantified using numeric features calculated from the frequency domain representation of the signal. Two basic features commonly used are the mean and median frequency.

The mean frequency of the power spectrum of a signal can be defined as a sum of products of frequencies and corresponding spectral values divided by the total power in the signal:

$$f_\mu = \frac{\sum_{i=1}^{N} f_i P_i}{\sum_{i=1}^{N} P_i},$$

where N is the number frequency bins, f_i is the frequency of bin i and P_i is the power of the spectrum at bin i. The median frequency is the frequency that divides the power spectrum into two equally powerful areas. To obtain the median frequency, the total power in the signal segment can first be calculated and divided by 2:

$$P_m = \frac{1}{2}\sum_{i=1}^{N} Pi\ .$$

The spectral values are then cumulatively summed until the value of P_m is exceeded. The frequency of the spectral component at which the threshold P_m is achieved is the median frequency.

Mean and median frequencies have several applications when observing the changes in signal properties. One of the most important applications of the median frequency has been to measure the depth of anesthesia. There is a close correlation between median frequency, the level of consciousness and the amount of anesthetic agents in the blood and brain (Schwilden 1989).

Spectral edge frequency

Spectral edge frequency (SEF x) represents the frequency below which x percent of the total power in the signal segment resides (Szeto 1990). Median frequency can therefore be considered as the special case of SEF 50.

Spectral edge frequency can be applied in a similar manner as the mean and median frequencies; to track changes in long-term EEG recordings per patient or to determine thresholds indicating normal levels in certain conditions. As the median frequency, SEF has been proposed as an indicator of the level on consciousness in depth of anesthesia assessment or of a sleep stage (Bruhn et al. 2003; Nieuwenhuijs et al. 2002).

Figure 9 presents several features derived from the frequency domain representation of an EEG signal. Absolute and relative powers of the EEG rhythms indicate a relatively strong (42%) alpha rhythm. The highest power peak of the signal (Peak power) is calculated to lie at the frequency of 9.1 Hz. Median frequency is one herz lower at 8.1 Hz and mean frequency at 7.6 Hz. The frequency of 24.8 Hz represents the calculated edge frequency leaving 95 % of the total power below. The SEF containing 95% of the area is commonly called as SEF 95.

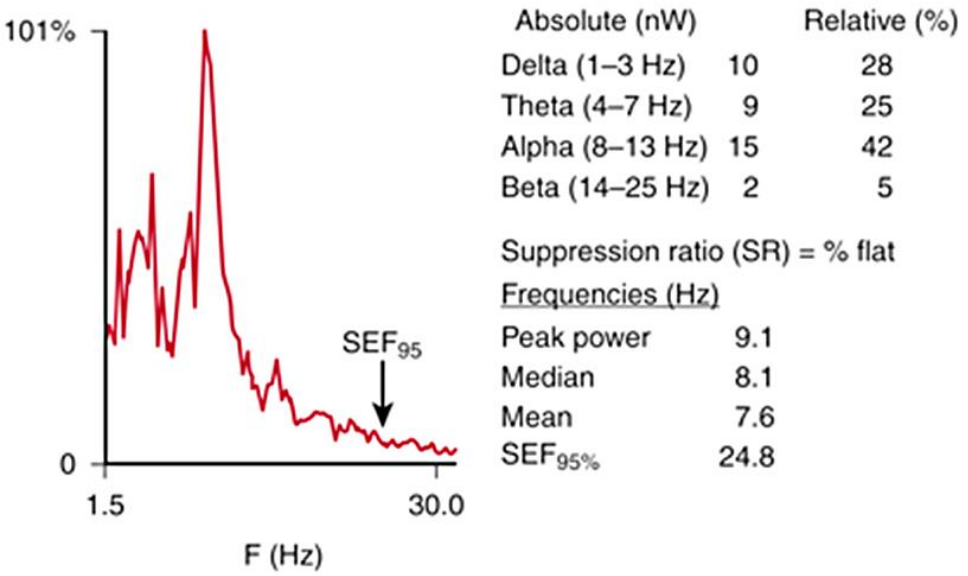

Figure 9. *An example of SEF 95 and other frequency domain features. Data is obtained from an anesthetized patient. Adapted from* (Kaplan 2008).

2.2.3 Continuous EEG monitoring in the ICU

Continuous monitoring of EEG has become a popular tool in evaluating the neurological functions in patients with critical brain or nervous system related conditions (Ney et al. 2013). Continuous monitoring of EEG in critical care is also referred as Critical Care Continuous EEG (CCEEG) (Herman et al. 2015). Noticeable results were found in a study reviewing the outcomes in mechanically ventilated patients monitored using cEEG vs. routine EEG. In this context, routine EEG refers to monitoring the patient for a limited period of time, say 30 minutes, for example, at a time. These routine measurements are commonly done repeatedly. The study was conducted in the United States during 2005-2009. In the study, the usage of cEEG was proven to result in a noticeably lower in-hospital mortality rate when compared to routine EEG without adding to the cost of hospital stay significantly (Ney et al. 2013).

In a review article by Jordan, five reasons are mentioned to encourage the usage of EEG monitoring in the ICU (Jordan 1993):

- EEG is linked to cerebral metabolism
- EEG is sensitive to hypoxia and ischemia, which are two of the most common causes of cerebral injury
- EEG correlates with cerebral topography and enables to localize abnormalities
- EEG deteriorates before irreversible cell damage, so it can be used to identify deteriorations and to intervene in time
- EEG is the best available method for detecting seizures.

Although the technology has advanced since the writing of the article, the claims are still viable. The following advantages and the conditions supporting the usage of cEEG in the ICU are listed in an overview article by Hirsch (Hirsch 2004):

- EEG is useful in the detection of subclinical seizures, especially in patients with certain conditions, including
    - fluctuating mental status
    - unexplained alteration of mental status
    - acute supratentorial brain injury with altered mental status
    - after convulsive status epilepticus.
- EEG is used to characterize spells, when patients are showing symptoms like
    - episodic posturing or other paroxysmal or repetitive movements
    - subtle twitching, nystagmus, eye deviation, chewing
    - paroxysmal autonomic spells including tachycardia.
- EEG is commonly used when assessing the level of sedation and following trends.
- EEG can be used to manage burst-suppression in anesthetic coma.
- EEG is useful for detecting ischemia in patients
    - after subarachnoid hemorrhage
    - during and after vascular neurosurgical or interventional neuroradiology procedures
    - with hemodynamic lesions and borderline flow
    - at risk for in-hospital acute ischemia.
- EEG is useful for prognostication.

The detection of seizures is considered as the single most important application of cEEG monitoring in the ICU. This is due to the fact that seizures in critically ill patients are mostly nonconvulsive and thereby difficult, if not impossible, to detect without monitoring devices. Based on several studies, approximately 20% of the patients under continuous EEG monitoring in the ICU have seizures. The number of seizures have been a matter of interest in several studies such as (Vespa et al. 1999), where 22% of monitored patients had seizures of which 52% were nonconvulsive and (Claassen et al. 2004), where 19% of the patients had seizures of which 92% were of the nonconvulsive type.

Similar ratio was found in an overview of multiple studies (Hirsch 2004). The studies by Vespa et al. and Claassen et al., mentioned above, were included in this overview. In total, 110 (19%) of 570 monitored patients combined from several studies had seizures during the monitoring. An important notice can be made that 88% of all the patients who had

seizures, had their first seizure during the first 24 hours of monitoring. However comatose patients were more likely to have the first seizure after the first 24 hours (Claassen et al. 2004).

In order to fully benefit from the cEEG, it is of high importance to define the findings that need to be addressed. American Clinical Neurophysiology Society has made an attempt to standardize the terminology (Hirsch et al. 2012). The paper includes a naming convention and exemplary figures of waveforms of interest as a guidance material for interpretation. The following listing describes the proposed nomenclature of patterns, a reference chart and figures of two example cases. More exemplary figures are available in (Hirsch et al. 2012).

The naming convention adopted in (Hirsch et al. 2012) is a hierarchic one, starting with a more general classification of the nature of the rhythm or pattern according to the following list:

- Generalized (G) referring to any bilateral, bisynchronous and symmetric pattern
- Lateralized (L) including unilateral and bilateral synchronous but asymmetric patterns
- Bilateral Independent (BI) referring to the presence of 2 independent (asynchronous) lateralized patterns, one in each hemisphere
- Multifocal (Mf) referring to the presence of at least three independent lateralized patterns with at least one in each hemisphere.

The general classification notion is followed by a term describing the actual phenomenon:

- Periodic Discharges (PDs): In this context, the term periodic refers to repetition of a waveform with relatively uniform morphology and duration with a quantifiable inter-discharge interval between consecutive waveforms and recurrence of the waveform at nearly regular intervals. Discharges are defined as waveforms with no more than 3 phases or any waveform lasting 0.5 seconds or less, regardless of the number of phases.
- Rhythmic Delta Activity (RDA): Rhythmic stands for repetition of a waveform with relatively uniform morphology and duration, and without an interval between consecutive waveforms. Delta activity refers to the frequency of the activity ($\leq$ 4 Hz).
- Spike-and-wave or Sharp-and-wave (SW): The term stands for a polyspike, spike or sharp wave consistently followed by a slow wave in a regularly repeating and alternating pattern, with a consistent relationship between the spike component and the slow wave; and with no interval between one spike-wave complex and the next.

These will then be complemented with modifiers that add details to the description of the finding. Modifiers used are, for example, duration, frequency, sharpness etc. All modifiers (plus, major and minor) are introduced in the reference chart (Figure 10).

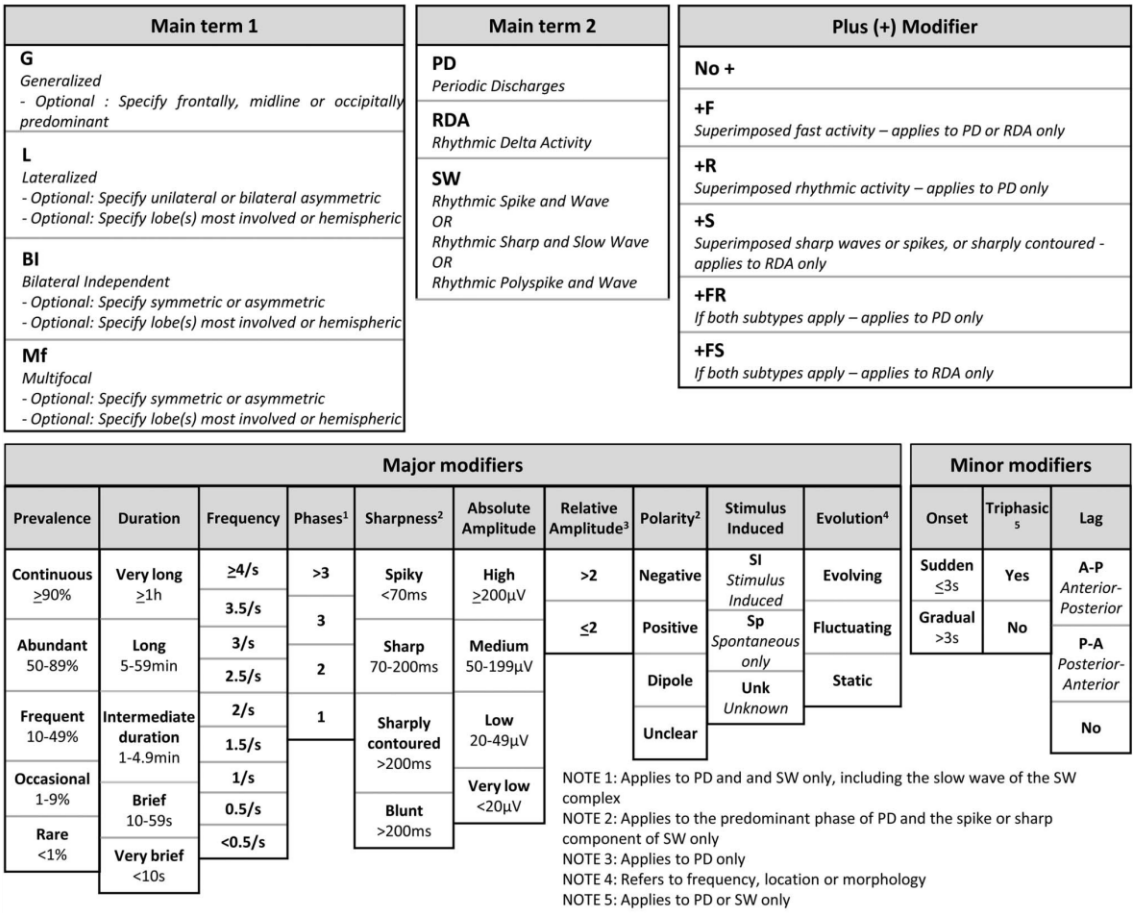

Figure 10. *2012 ACNS CCEEG terminology reference chart* (Hirsch et al. 2012).

Two exemplary figures using the naming convention introduced above, were selected to be presented here. Figure 11 shows sharply contoured lateralized periodic discharges, where discharges are bilateral asymmetric. Using the hierarchical classification and the modifiers presented above, the Main term 1 for this class of patterns is ‘Lateralized’ (L), Main term 2 is ‘Periodic discharge’ (PD) and the only modifier used is the major modifier ‘Sharply contoured’. Using the same classification principle, Figure 12 represents a Generalized Spike-and-wave (GSW) pattern. (Hirsch et al. 2012)

Figure 11. *Sharply contoured lateralized periodic discharges where periodic discharges are bilateral asymmetric.* (Hirsch et al. 2012).

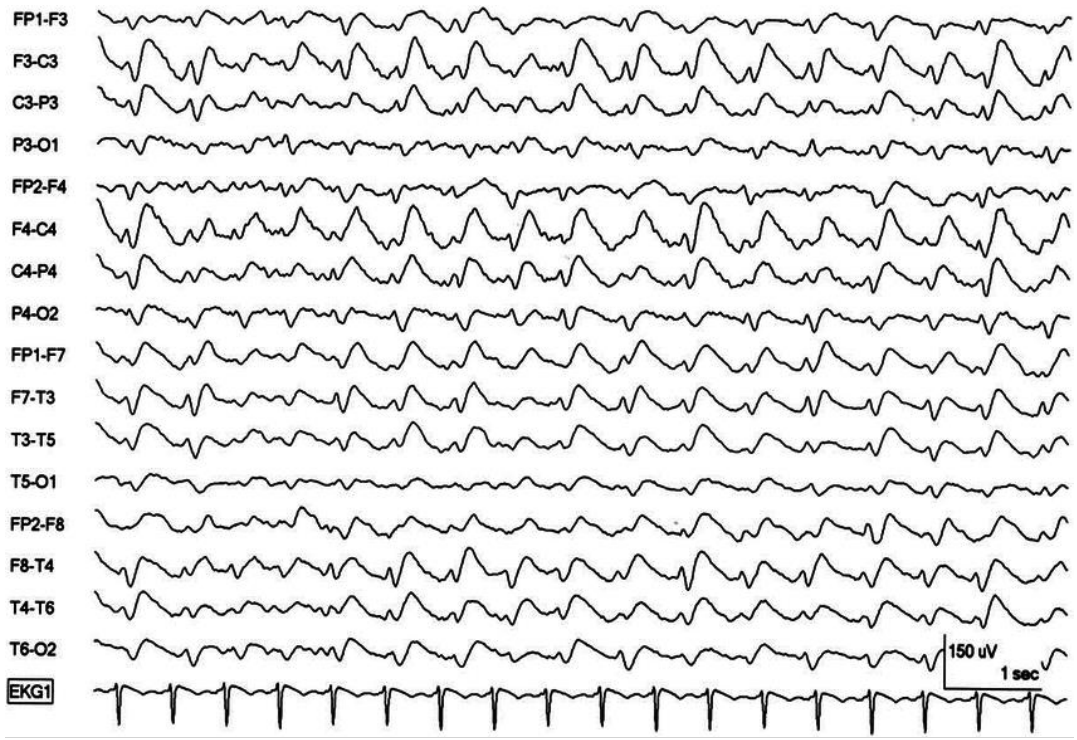

Figure 12. *Generalized spike-and-wave* (Hirsch et al. 2012).

The interpretation of the abnormalities is not always straightforward. Common terminology and basic guidance for interpretation and classification adds to comparability between different studies and allows to create treatment plans based on findings.

Despite this kind of common terminology, there is no clear consensus of which patterns need immediate treatment and how aggressively, if at all, those should be treated. The actual effect of treating seizure-like conditions using anti-seizure medication in comatose

patients on the outcome of the treatment also remains unclear (Trinka & Leitinger 2015). In a recent study, patients having 2 or more periodic discharges (PDs) per second were found to benefit from anti-seizure medication (Witsch et al. 2017).

2.2.4 Artifacts

Artifacts can be described as corruption in the measured data. As EEG measures extremely low voltages and their alterations, even the smallest disturbances affect the outcome of the measurement. Artifacts can roughly be categorized as internal or external. External artifacts occur as a result of some phenomenon or event external of the subject. For example, a poor attachment of an electrode causes an external artifact that results in high potential differences or, if the electrode detaches, in zero potential difference. Internal artifacts are the result of something the subject being measured does intentionally or unintentionally. Typical internal artifacts are triggered by eye or facial muscle movement, electrocardiogram and subject's own skin potential. As there are different sources of artifacts, the types of the artifacts also differ. The characteristics of some internal and external artifacts are easily recognizable by an expert, but in uncertain cases caution is advised in order not to mistake a serious abnormality for an artifact.

The number of different artifact types is too large to be introduced in the scope of this work, however, some common types of internal artifacts are presented to illustrate the irregularities considered as artifacts.

Cardiac artifact

The electrocardiography (ECG) artifact is a disturbance caused by the patient's heartbeat. ECG artifacts can be removed quite reliably using computational algorithms, especially, if the ECG has also been recorded or is being monitored in real-time. In Figure 13, the lower graph represents the pure ECG signal and the top graph is a single channel of EEG corrupted by the ECG signal.

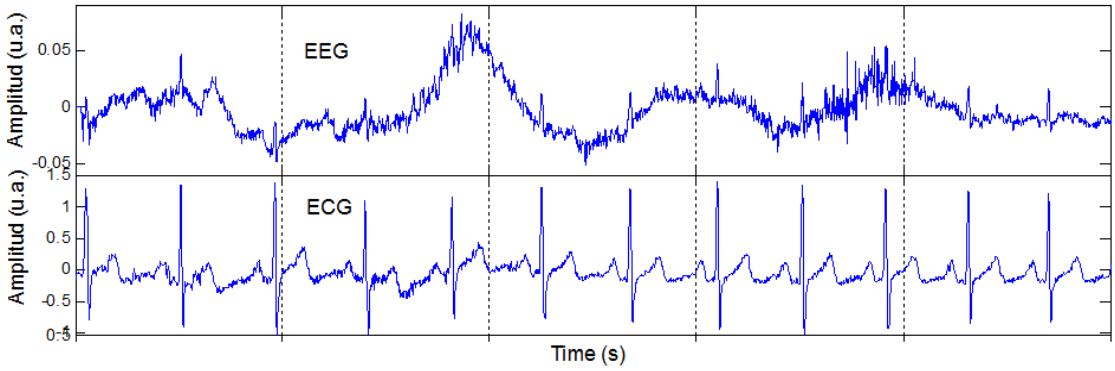

Figure 13. *EEG-signal including cardiac artifacts and ECG signal as a reference. Adapted from* (Garces Correa & Laciar 2011).

Ocular (EOG) artifact

Ocular artifacts are caused by eye movements, including blinking. In case of conscious patients, a common technique of minimizing the amount of eye movements and blinking is to have the patient wear eye blinders (Klass 1995). This is done in order to remove the external stimulus that could cause artifacts. The EOG, when monitored, can be used as a reference when observing the ocular artifacts. The top graph of Figure 14 contains a single channel EEG with EOG artifacts along with spike-formed ECG artifacts. On the bottom graph, an EOG is presented as a reference signal.

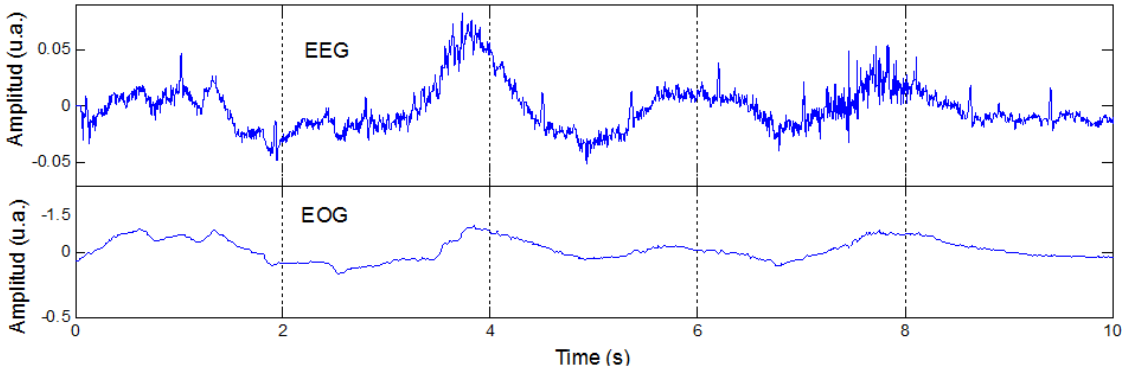

Figure 14. *EOG artifacts in the EEG along with ECG-artifacts. Adapted from* (Garces Correa & Laciar 2011).

Muscular artifacts

Muscular artifacts (EMG) are a result of intentional or unintentional muscle contractions. Although muscle artifacts can be found at lower frequencies, they most commonly appear in the frequency band of ~20-300 Hz and can be easily mistaken as high frequency brain activity (Muthukumaraswamy 2013). Muscular artifacts as all artifacts come in many forms and variations. In Figure 15, a rare muscle artifact with increased power at the high end of the spectrum is shown.

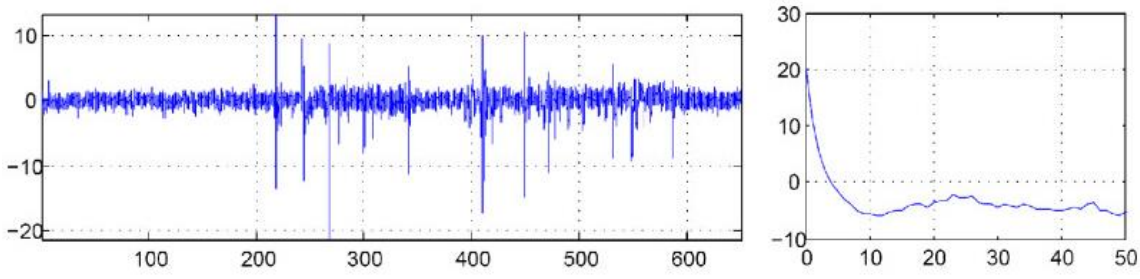

Figure 15. *A muscle artifact with increased power at the high end of the spectrum* (Winkler et al. 2011).

2.2.5 Techniques for artifact detection and removal

Besides manual inspection, various automatic and semi-automatic methods have been studied and implemented in order to automate the artifact detection and removal procedure. The simplest automatic methods monitor amplitude or signal power in a moving window and compare the values to either predefined or adaptive threshold levels.

In recent years, as computational algorithms and power have increased in efficiency and reduced in cost, more advanced methods have been developed. These methods can be automatic or semi-automatic depending on their need for human intervention. The semi-automatic methods can be used as pre-detectors, the work of which an expert will confirm. Automatic methods are used to directly remove artifacts with no human intervention. Main problems in the automation of artifact detection derive from different artifact types requiring different rulesets of recognition. Also, some abnormalities of brain function cannot be reliably separated from artifacts.

More advanced automated and semi-automated artifact detection and removal tools are based on statistical models, neural networks and other classifiers. Commonly the tool is a combination of several techniques. A popular method of analysis used in these tools is the Independent Component Analysis (ICA) and its derivatives such as the wICA that is a combination of wavelet transform and the ICA. WICA has been successfully used in automatic ECG artifact rejection in (Taelman et al. 2007; Calcagno et al. 2014), for example.

2.3 Treatment of traumatic brain injury in the intensive care unit

Traumatic brain injury (TBI) is usually caused by a sudden damage to the brain. The severity level of brain injury can be categorized as mild, moderate or severe. The severity is commonly measured using the Glasgow Coma Scale (GCS) that was implemented in 1974 as a result of a study by Teasdale and Jennett (Teasdale & Jennett 1974). The scale has had some minor changes since its introduction and it has been found to be a valuable tool for clinical assessment of brain injury patients (Teasdale et al. 2014).

GCS is assessed by scoring the results of three responsivity tests (Table 2). The sum of the scores gives an overall picture of the severity of the test subject's brain injury while the sum of each test must also be considered separately. As stated in an article by the inventor of GCS "*Individual patients are best described by the three components of the coma scale; whereas the derived total coma score should be used to characterize groups*" (Teasdale et al. 2014).

Table 2. *Glasgow Coma Scale scoring adapted from* (Teasdale et al. 2014).

Eye opening	**motor response**	**verbal response**
4: Spontaneously 3: To sound 2: To pressure 1: None	6: Obeys commands 5: Localizing 4: Normal flexion 3: Abnormal Flexion 2: Extension 1: None	5: Orientated 4: Confused 3: Words 2: Sounds 1: None
Sum of points	Sum of points	Sum of points
Sum of points		

The knowledge of the state of a TBI patient's awareness and brain functionality gives major insight for the doctors treating the patient. For example, if the patient is suffering from nonconvulsive seizures, the information obtained from EEG monitoring helps the treating faculty to choose the right medicines at the right time. EEG can be used as a tool to monitor the progress of the patient's responsiveness to treatment and rest. Without the capability of EEG monitoring, when patients are being held in medically infused coma, they are repeatedly woken up from the coma to assess the functionality of the brain and the progress of the treatment.

There are several studies proposing different ways of predicting the outcome of TBI patients based on the changes in wave patterns and different features calculated from the EEG recordings. Repeated recordings or constant monitoring of the EEG are used to study changes in the patient's brain function and the features calculated from the recordings can be used to categorize the patient.

While GCS is used to assess the severity of the brain damage, another scale, the Glasgow Outcome Scale (GOS), is used to predict or document the outcome of the treatment. The scale divides the outcomes into five categories: death, persistent vegetative state, severe disability, moderate disability and good recovery (Jennett & Bond 1975). The original version of the GOS received critique due to having only five categories and therefore not providing detailed information about the disability level. An Extended version of GOS (GOSE) was introduced to overcome the limitations of the five-point scale by subdividing the disability and recovery categories to provide more detailed (8-point) information (Jennett et al. 1981). GOSE is recommended to be used instead of the GOS despite the additional effort of the assessment. GOSE should be preferred due to its ability to provide higher statistical efficiency when compared to GOS (Weir et al. 2012). GOSE is the recommended method of assessing the outcome of severe head injury (Teasdale et al. 1998). Table 3 shows the difference between the original GOS and the GOSE. The extension divides the classifications of conscious survivors into two sublevels each.

Table 3. *Classification of disability due to brain damage (conscious survivors). Adapted from* (Jennett et al. 1981).

Acute brain damage (traumatic or not)

Glasgow Scale Jennett and Bond (1975) 3 point	Glasgow Scale Jennett and Bond (1981) 6 point
Severe disability (3)	5
	4
Moderate disability (2)	3
	2
Good recovery (1)	1
	0

3. EEG-BASED BRAIN CONNECTIVITY AND NETWORK ANALYSIS

The connectivity between EEG channels or areas of the brain has been widely studied and has given promising results in analyzing and predicting certain brain and nervous system related illnesses.

3.1 Synchronization and coupling

There are multiple methods that can be used to study the human brain using the EEG. Of these methods, synchronization and coupling of the activity between various brain regions have gained a lot of interest recently. For example, synchronization and coupling have been successfully used to evaluate and diagnose Mild Cognitive Impairment (MCI), which has been associated with the risk of the Alzheimer disease at its early stages (Wen et al. 2015).

3.1.1 Cross Frequency Coupling

Cross frequency coupling can be described as an interaction between oscillations of different frequency bands. The coupling effect can be studied in different forms, depending on the objectives of the study. The phenomenon can be observed as some combination of frequency, amplitude and phase. The most common coupling effects are the power-power, phase-phase, phase-frequency and phase-power (or phase-amplitude) couplings. Figure 16 illustrates the outcomes of different types of coupling effects between two given signals.

While observing the EEG data and in neuroscience in general, one of the commonly studied coupling effects is the phase-amplitude coupling (PAC). Phase-amplitude coupling refers to a technique, where the modulation of the amplitude of a higher frequency component by the phase of a lower frequency component of either the same signal or a signal measured from a different channel is investigated. Several different frequency band combinations have been studied and have given positive results in various contexts. However, there is no standardization or subsequent proof that would emphasize certain frequency ranges. Commonly, the frequency bands used in studies are those corresponding to conventional EEG rhythms (alpha, beta, delta and theta) or sub-bands of those, such as the lower delta, for example.

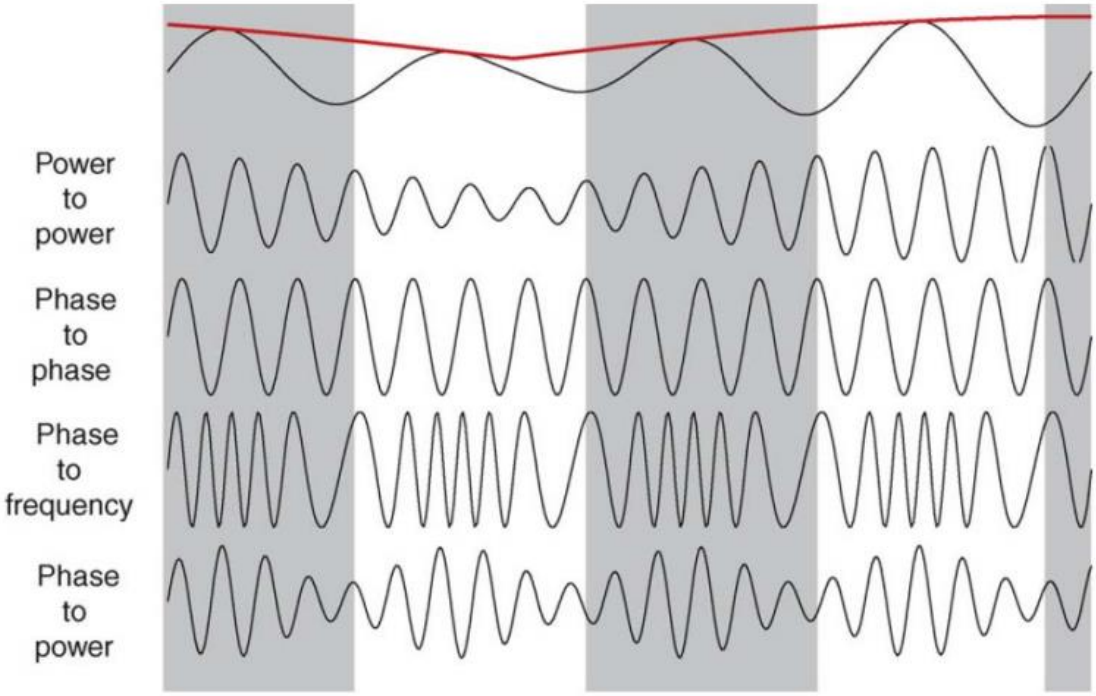

Figure 16. *Outcomes of different types of cross-frequency coupling* (Jensen & Colgin 2007).

There are several methods for quantifying coupling effects. None of these has become dominant so that it could be considered as the de facto definition of the coupling phenomenon. One of the common measures frequently used is the Phase Locking Value (PLV). Originally PLV was introduced to directly quantify frequency-specific synchronizations between two signals (Lachaux et al. 1999). The basic principle can also be used to measure the phase-amplitude coupling by, instead of calculating the value based on two phases directly (phase-phase), the phase of the amplitude envelope of a higher frequency band is used instead (phase-amplitude) (Penny et al. 2008).

The procedure to measure the PAC using the PLV principle can be described by the following steps:

1. low-pass filtering of the modulating component
2. using the Hilbert transform to obtaining the phase of the modulating component from step 1
3. filtering the signal tested for being modulated to extract the higher frequency component
4. deriving an amplitude envelope of the high frequency signal from step 3
5. extracting the phase of the amplitude envelope using the Hilbert transform
6. calculating the phase locking value between the results of steps 2 and 5:
   $PLV = \left\| \langle \exp[i\left(\phi_{f_p} - \phi_{A_{fA}}\right)] \rangle \right\|,$

where ϕ_{f_p} is the phase of the lower frequency component, $\phi_{A_{fA}}$ is the phase of the amplitude envelope of the higher frequency component and $\langle\cdot\rangle$ is the mean over the sample points and $\|\cdot\|$ is the length of the mean vector (Tort et al. 2010).

PLV returns a value between 0 and 1, where 0 represents the lack of synchronization (complete desynchronization) and 1 translates to completely locked series of phase differences. In the following, the measure obtained using the above algorithm is referred to as the PAC/PLV measure indicating the assessment of phase-amplitude coupling using the phase locking value principle.

3.1.2 Coherence

Coherence describes linear association between two signals as a function of frequency. When comparing two EEG signals, the output should be normalized so that the results are comparative. Therefore, magnitude squared coherence, normalized by the product of the autospectra of the two signals is commonly used as it is automatically normalized between 0 and 1. The magnitude squared coherence function can be defined as:

$$Coh_{xy}(f) = \frac{|S_{xy}(f)|^2}{S_x(f)S_y(f)},$$

where $S_{xy}(f)$ is the cross-power spectrum between signals x and y, $S_x(f)$ is the autospectral density of the signal x and $S_y(f)$ is the autospectral density of the signal y.

3.2 Brain as a network

Human brain can be considered as a network and therefore it can be studied using the tools provided by graph theory. In general, all systems that contain objects or areas that are somehow linked to each other can be studied and analyzed this way. The true amount of neurons (nodes) in the human brain cannot be exactly measured, but it has been estimated to be in a range of 86.1 ± 8.1 billion (Azevedo et al. 2009). These neurons form a network that cannot itself be studied directly, instead, when forming graphs of the brain data regardless of the measurement technique (EEG, MEG etc.) we are creating a network of integrated brain activity rather than connectivity of individual neurons.

Depending on the application, the network can consist of either binary or weighted connections. A network is considered binary when the connections between nodes either exist or not and weighted, if the magnitude of the connection is important. Either weighted or binary, connections between nodes on a network may be directed or undirected. The directed network consists of connections (edges) associated with direction while the connections in an undirected network have no directionality. On a directed weighted network,

the values of connections may therefore differ depending on the direction of the connection. For example a network formed of a PAC/PLV connectivity matrix is weighted and directed and a network derived from a coherence based connectivity matrix is weighted an undirected due to the nature of coherence.

3.2.1 Connectivity matrix

Considering the brain regions (corresponding, in our case, to electrode locations) as parts of a network allows to create a matrix of data that contains the calculated measures of each region pair at a given period of time. In graph theory, this matrix would be referred to as the adjacency matrix. Depending on the measurement and the needs of the study, each measurement can refer to a time span that best describes the phenomenon being studied. The adjacency matrix can be used to create a visual interpretation of the connectivity between the areas of measurement or of combined measurements. This connectivity mapping containing the connectivity measures is referred to as the connectome in brain network analysis (Sporns et al. 2005). For example, if using 19 EEG channels as the data source for calculations, the outcome would be a sequence of 19x19 matrices. Each matrix would contain the connectivity data for a certain time span. Knowing the positions of the electrodes, the electrodes can be grouped by brain regions and averaged to create smaller matrices describing different brain segments (Joudaki et al. 2012). An example of a connectivity matrix is introduced in Figure 17 and its visual representation in Figure 18. The matrix consists of PAC/PLV data calculated in a time span of 120 seconds using frequency bands of 0-2 Hz and 8-13 Hz.

	Fp1	Fp2	F7	F3	Fz	F4	F8	T3	C3	Cz	C4	T4	T5	P3	Pz	P4	T6	O1	O2
Fp1	0,078	0,068	0,050	0,045	0,067	0,028	0,026	0,071	0,009	0,036	0,019	0,020	0,033	0,040	0,037	0,052	0,041	0,089	0,042
Fp2	0,043	0,064	0,036	0,010	0,067	0,053	0,019	0,071	0,046	0,042	0,055	0,054	0,047	0,047	0,045	0,044	0,031	0,058	0,053
F7	0,024	0,026	0,049	0,014	0,059	0,043	0,006	0,032	0,034	0,016	0,007	0,052	0,034	0,025	0,007	0,059	0,041	0,058	0,027
F3	0,100	0,095	0,080	0,099	0,094	0,037	0,060	0,006	0,067	0,052	0,044	0,046	0,019	0,049	0,041	0,029	0,034	0,024	0,020
Fz	0,106	0,092	0,094	0,048	0,133	0,057	0,063	0,058	0,062	0,032	0,059	0,045	0,035	0,010	0,014	0,031	0,033	0,056	0,009
F4	0,023	0,056	0,004	0,011	0,062	0,058	0,041	0,025	0,023	0,008	0,032	0,009	0,030	0,014	0,020	0,019	0,023	0,063	0,012
F8	0,039	0,052	0,034	0,033	0,045	0,054	0,020	0,057	0,036	0,026	0,046	0,052	0,045	0,054	0,073	0,069	0,052	0,058	0,049
T3	0,018	0,032	0,020	0,041	0,027	0,041	0,051	0,017	0,025	0,048	0,023	0,056	0,022	0,037	0,033	0,027	0,042	0,041	0,030
C3	0,020	0,027	0,022	0,028	0,016	0,015	0,023	0,030	0,026	0,039	0,020	0,005	0,014	0,023	0,048	0,036	0,024	0,058	0,032
Cz	0,032	0,038	0,036	0,026	0,041	0,044	0,054	0,039	0,060	0,100	0,045	0,059	0,033	0,041	0,105	0,084	0,049	0,084	0,064
C4	0,043	0,023	0,017	0,030	0,046	0,044	0,045	0,014	0,029	0,054	0,068	0,027	0,033	0,020	0,046	0,051	0,019	0,029	0,026
T4	0,051	0,045	0,016	0,049	0,023	0,036	0,029	0,041	0,018	0,016	0,040	0,064	0,049	0,013	0,031	0,041	0,007	0,054	0,022
T5	0,017	0,028	0,027	0,025	0,012	0,048	0,055	0,051	0,032	0,028	0,043	0,066	0,054	0,067	0,054	0,049	0,050	0,088	0,057
P3	0,005	0,021	0,009	0,018	0,016	0,037	0,010	0,050	0,036	0,008	0,024	0,027	0,050	0,060	0,026	0,009	0,017	0,052	0,056
Pz	0,044	0,043	0,040	0,032	0,032	0,011	0,024	0,032	0,058	0,055	0,028	0,036	0,059	0,048	0,031	0,066	0,039	0,047	0,032
P4	0,056	0,052	0,035	0,025	0,031	0,060	0,019	0,039	0,026	0,046	0,037	0,046	0,031	0,016	0,022	0,062	0,050	0,005	0,033
T6	0,062	0,071	0,051	0,037	0,048	0,054	0,030	0,028	0,036	0,015	0,031	0,041	0,039	0,020	0,039	0,038	0,060	0,023	0,041
O1	0,074	0,093	0,074	0,090	0,048	0,076	0,059	0,086	0,051	0,064	0,062	0,087	0,070	0,040	0,053	0,048	0,058	0,041	0,068
O2	0,021	0,016	0,031	0,029	0,033	0,023	0,040	0,036	0,061	0,071	0,063	0,035	0,041	0,020	0,045	0,050	0,054	0,012	0,086

Figure 17. *PAC/PLV connectivity matrix of a 120 s data segment.*

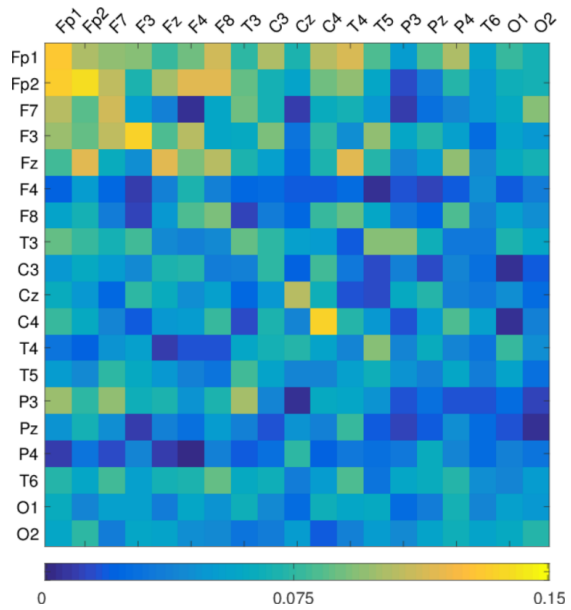

Figure 18. *Visual representation of the connectivity matrix in Figure 17. Warm color indicates higher value and colder color lower values as presented in the color bar.*

3.2.2 Connectivity graph

The data in the adjacency matrix may be directed or undirected depending on the methods used to capture the coupling or synchronization effects. When using methods that produce directional data, the adjacency matrix can be used to create a directed graph containing the coupling effects from each brain region to any other. Using the terminology of graph theory, brain regions are called nodes, the connections between the brain regions are referred to as edges and the value related to each connection between brain regions (the values in the matrix) would be considered as weights. A simple example of a graph based on the adjacency matrix (Figure 19) shows the basic principle behind graph formation. In this example, the coupling measure is the PAC, hence each row of the adjacency matrix represents the modulating EEG channel and each column corresponds to the channel being modulated. The values in the matrix are the PAC measures calculated based on the signals measures at corresponding electrodes.

It is important to notice that this is a fully connected graph and no threshold value has been used to separate or classify the magnitude of the connectivity. Thresholding is necessary in some applications in order to find meaningful connections to be converted into edges (van Wijk et al. 2010). Removing all connections below the selected threshold level leads to a graph where all the remaining connections are significant. When thresholding the example graph of Figure 19 to contain connections with a value larger than 0.1, only two connections (besides loops) remain (Figure 20): from F7 to Fp1 and from Fp1 to Fp2.

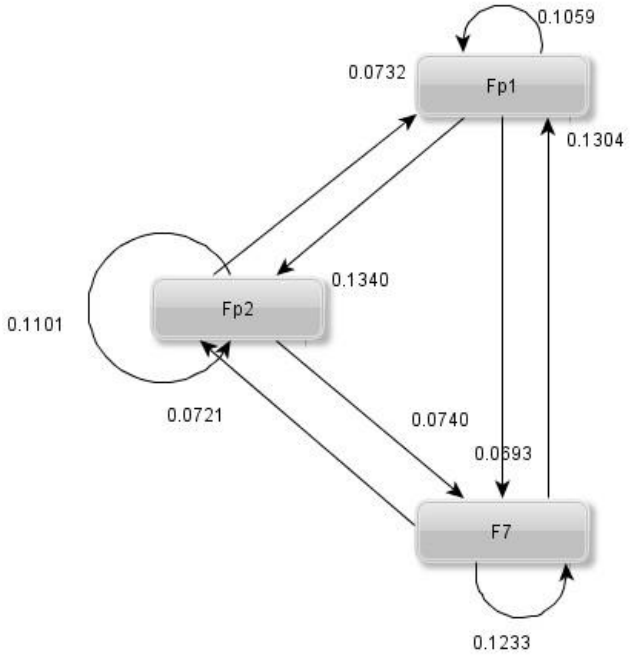

	Fp1	Fp2	F7
Fp1	0.1059	0.1340	0.0693
Fp2	0.0732	0.1101	0.0721
F7	0.1304	0.0740	0.1233

Figure 19. *A graph derived from a PAC based connectivity matrix of three EEG channels. Frequency ranges used are 0-2 Hz → 8-13 Hz*

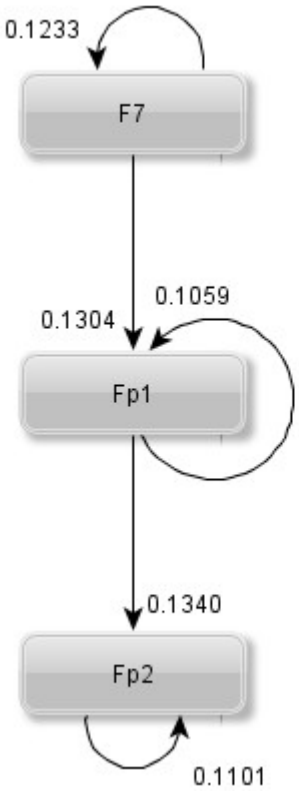

	Fp1	Fp2	F7
Fp1	0.1059	0.1340	0
Fp2	0	0.1101	0
F7	0.1304	0	0.1233

Figure 20. *A thresholded (0.1 as the limit) version of the graph in Figure 19.*

3.3 Measures of a brain network

The graph derived from the measures of synchrony or coupling between EEG channels can be seen as a visual representation of the interactions between the brain regions. This information can be used to calculate various properties of the brain network such as degree, clustering coefficient or small-worldness, for example. These and several other measures can be used to quantify the effectiveness, modularity or connectivity properties of the (brain) network. The following sections describe the three measures implemented in the toolbox created during this thesis.

3.3.1 Degree

Degree represents the number of edges that connect a node to other nodes. In the case of a directed graph, this value may contain information on incoming connections or outgoing connections. Total (a sum of in and out degrees) degree can also be used as a measure to get a general, undirected view of the connections. Knowing the number of nodes in the network, the method may also be used to present the distribution of degrees. This can be useful to assess the probability of a random node having a given degree. Calculating the total degree probability $P(d)$ of our example graph (Figure 20) gives probabilities $P(3) = 2/3$ and $P(4) = 1/3$ as self-loops are counted twice. With the example graph being small with only three nodes, the distribution of the total degree can be easily seen without further calculation.

Another interesting expansion of the concept of degree is the degree correlation. Degree correlation observes the connection mixing according to the degrees of nodes (Newman 2003).

3.3.2 Clustering coefficient

Like degree, the clustering coefficient measures the connectivity or cohesion of the network. The basic principle behind the clustering coefficient is to count connected triangles of the network (global clustering coefficient) or of a single node (local clustering coefficient). Clustering coefficient can be calculated for weighted or binary networks. The simplest example would be the calculation of the clustering coefficient for a binary undirected network. The local clustering coefficient of such a network would simply be calculated by summing the pairs of node x's neighbors that are also connected to each other. This sum is normalized by the total number of pairs connected to node x and expressed as

$$C(x) = \frac{t_x}{Nc},$$

where t_x denotes the number of node pairs connected to each other and to node x (triangles) and Nc denotes the number of node pairs connected to the node x. For a binary

undirected network, the number of pairs connected to node x (Nc) can be expressed using the number of connections (degree):

$$Nc = \frac{1}{2} k_x(k_x - 1) ,$$

where k_x is the number of connections (degree) of the node x. Thereby the clustering coefficient formula for the binary undirected network can be written as

$$C(x) = \frac{2t_x}{k_x(k_x - 1)} .$$

This can also be considered as the probability of node x's neighbors to be connected with each other (Fornito et al. 2016).

One form of the global clustering coefficient follows the same basic principle of counting the triangles and dividing the sum by the number of all possible triangles. The first reference to a similar measure is from 1949 (Luce & Perry 1949). There are two methods used to calculate the global clustering coefficient. The original version published in 1998 suggests the clustering coefficients of individual nodes to be averaged over the number of nodes (Watts & Strogatz 1998). This results in a formula where the sum of local clustering coefficients is normalized using the total number of nodes:

$$C = \frac{1}{N} \sum_{x \in N} \frac{2t_x}{k_x(k_x - 1)} .$$

In some contexts this is referred to as the mean clustering coefficient or as the network-wide clustering coefficient (Fornito et al. 2016), while in other contexts as a method of calculating the global clustering coefficient (Soffer & Vázquez 2005).

Normalization used in the above equation leads to biased results when the network contains nodes with small amounts of connections. In this case, the denominator of terms corresponding to these nodes will be small and hence the calculation method adds weight to nodes with less connections (Fornito et al. 2016). To balance the weights, another method of calculating the global clustering coefficient is commonly used. In some publications this method is referred to as transitivity, global transitivity or transitivity coefficient. Instead of calculating the summation of each local clustering coefficient, the numerator and the denominator are summed individually over all nodes before the division:

$$C = \frac{\sum_{x \in N} 2t_x}{\sum_{x \in N} k_x(k_x - 1)} .$$

Another commonly seen, less mathematical way of describing the calculation method literally is

$$C = \frac{3x\ number\ of\ triangles\ (closed\ triplets)}{number\ of\ triplets}.$$

Simply put, the numerator represents the number of triangles formed by nodes and the denominator includes the number of three node groups where at least one of the nodes is connected to both of the remaining nodes. For example, in a network containing nodes n1, n2 and n3, a triplet is formed when there are edges (n1, n2) and (n2, n3). If the edge (n1, n3) exists, the triplet is a triangle (closed triplet) as well (Newman et al. 2002).

Both of the previously introduced methods for the calculation of the global clustering coefficient have been used in several studies. The used calculation methods need to be taken into consideration when comparing the results of different studies because they are not fully comparative.

The calculation of the clustering coefficient based on weighted graphs needs an additional value of the triplets to be defined. This value describes the combined weight of the triplet. There are several methods used to calculate this value such as arithmetic mean, geometric mean, maximum and minimum. Examples of the triplet calculation methods can be seen in Table 4.

Table 4. *Methods for calculating the triplet value, ω. Adapted from* (Opsahl & Panzarasa 2009)

Method	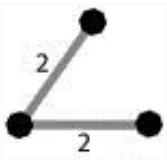	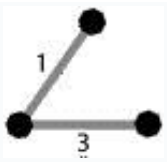
Arithmetic mean	$(2+2)/2 = 2$	$(1+3)/2 = 2$
Geometric mean	$\sqrt{2*2)} = 2$	$\sqrt{1*3} = 1{,}73$
Maximum	$max\ (2{,}2) = 2$	$max\ (1{,}3) = 3$
Minimum	$min\ (2{,}2) = 2$	$min\ (1{,}3) = 1$

The concept of generalized clustering coefficient was proposed to unify the calculation methods between weighted and binary networks. The generalized version relies on the values of connections instead of their number and is defined as

$$C_\omega = \frac{total\ value\ of\ closed\ triplets}{total\ value\ of\ triplets}.$$

The generalized version could be used with either binary or weighted networks. The results on binary networks would be equal to the result of the standard calculation method

as each connection would have a value of 1. Any of the triplet calculation methods may be used to calculate the proposed generalized clustering coefficient (Opsahl & Panzarasa 2009).

As a result of global clustering coefficient calculation, a single numerical value is produced. The value represents the network's level of clustering/cohesion normalized between 0 and 1. As a measure of cohesion, the clustering coefficient has been widely used in network studies and is considered as one of the most widely used characteristics of complex network theory (Saramäki et al. 2007).

3.3.3 Shortest path

Shortest path is the shortest possible route to connect two nodes in a graph. In binary networks, the shortest path determines the smallest amount of transitions between two nodes in order for those two nodes to be connected. This is due to the fact that each weight or cost between traveling from a connected node to another is always 1. This is not the case in weighted networks. In weighted graphs, the shortest path calculation must take into consideration the sum of weights at each path and compare these sums to conclude which of the paths is the shortest.

The average shortest path is calculated as the sum of the shortest paths between all node pairs normalized by the number of all possible node pairs. This can be expressed as

$$L = \frac{1}{N(N-1)} \sum_{i \neq j} L(i,j) \,,$$

where N is the number of nodes and $L(i,j)$ represents the shortest path from node i to node j. The average shortest path is commonly used to describe the connectivity of the network. The directionality of the network needs to be taken into consideration when calculating the shortest path as there might be differences between connections depending on the direction of the connection (Newman 2010).

3.3.4 Small-worldness

The idea behind the small-world networks is old and was formally introduced by Stanley Milgram. He studied the number of people needed to connect two random persons to each other via acquaintances and friends in order to deliver a message from the sender to the receiver (Milgram 1967).

The same phenomenon has been widely used to study real-life networks. The functional significance of real-life small-world networks was presented in a study, where the spreading of an infectious disease was used to test the theories behind the phenomenon. A network is considered a small-world network when it is highly clustered and the average

shortest path length is considered low. In other words, in a small-world network certain nodes act like hubs connecting groups of nodes together with paths that can be considered short. The properties used to assess small-worldness are the path length L and the clustering coefficient C. These values are then compared to the values calculated for a random graph containing the same number of nodes as the original graph. The small-world phenomenon can then be seen in a particular network if it's L is greater or close to that calculated for a comparative random graph and C is significantly larger than that calculated for a random network: $L >\approx L_{random},\ C \gg C_{random}$. (Watts & Strogatz 1998)

This method results in a binary interpretation of the small-world phenomenon: either the network has the small-world property or not. There is no distinction according to the magnitude of the phenomenon, which in many cases would be a matter of interest. A method for quantifying the effect was introduced to enable the comparison between networks. Quantification uses the same basic principles of the shortest path and clustering coefficient and their relation to their counterparts calculated for random graph:

$$C_\Delta = \frac{C}{C_{random}}\ , \qquad L_\Delta = \frac{L}{L_{random}}\ .$$

Values obtained from dividing the graph's measures by the ones for a random graph are then used to create an indicator of their ratio

$$S_\Delta = \frac{C_\Delta}{L_\Delta}.$$

As introduced earlier, a network is considered a small-world network when the clustering coefficient is significantly greater than the one for a random graph and the shortest path is close to that of the random graph. As a result of this statement, in the case of a small-world network, the denominator would be close to or slightly above 1 and the numerator would be far greater than 1. Using this information, a quantitative limit can be set and a network can be considered a small-world network when $S_\Delta > 1$. In addition, the magnitude of the value correlates directly with the magnitude of the small-world phenomenon in the network (Humphries & Gurney 2008).

3.4 Applications of EEG based network analysis

The number of applications using graph theory based network analysis of EEG has increased as the computational power and technologies have advanced. Applications and interpretations of complex network measures of brain connectivity are reviewed in an article by Rubinov and Sporns (Rubinov & Sporns 2010). The article contains many good references to applications in the field. In the following, some studies published after the article are briefly described.

In a study released in 2010, schizophrenic patients had their EEG recorded while performing a 2-back memory task. These recordings were used to calculate spectral coherence, which was used to create a network and to calculate node degree and the network density measure, which refers to total number of links compared to all possible links. Among other findings, it was noticed that when compared to a control group, the schizophrenic patients had significantly higher variability in their brain networks during the task. Another finding showed asymmetric values of node degree when succeeding in the memory tasks. (De Vico Fallani et al. 2010)

Certain network measures have been found to change during the maturation of the human brain. In a study by Boersma et al., EEG of 227 children between ages 5 and 7 was recorded and used to create directed graphs using the synchronization likelihood factor. The measurements indicated that as the brain matured, the properties of the brain derived network changed from random-like towards more organized small-world functional network. (Boersma et al. 2011)

Functional connectivity graphs (FCG) were created of cross-frequency phase interactions to classify correctness of working memory tasks in a study by Dimitriadis et al. Based on tensor subspace analysis (TSA), a correctness level of 96 % was achieved. Calculations required by the classifier were determined to be efficient enough, so that the methodology could be used in real-time applications. (Dimitriadis et al. 2015)

In a study by Vecchio et al., post-seizure EEG data of 30 stroke patients were studied using methods of connectivity analysis. The results were compared to the lesional volumes, which were obtained using Magnetic Resonance Imaging (MRI). The volume of lesions was found to correlate positively with the amount of clustering and path length in the lower frequency bands (delta and theta) and negatively in the lower alpha band. (Vecchio et al. 2016)

A recent preliminary study used an EEG based tool called Brain Network Activation (BNA) to assess brain functions in young athletes with concussions. The results were promising as significant reductions in BNA scores were detected in subjects above 16 years of age after the injury (concussion). The method itself uses a priori data to generate a reference brain network, which is then compared to the brain network of the subject. This study supports the use of the method to assess the changes in brain network after sports-related concussions, especially in patients over 16 years of age. (Reches et al. 2017)

4. BRAIN NETWORK ANALYSIS TOOLBOX

In this thesis, the main focus was on creating a working prototype of a modular toolbox for network analysis of multichannel EEG recordings. The toolbox was implemented using Matlab as the platform and the coding language. The toolbox was designed to be modular in the sense that parts of the toolbox can be used individually and the data may flow through the modules of the toolbox or, alternatively, external data can be used at any point.

Due to the prototypical nature of the toolbox, the programming methodology was not strictly determined and a mix-up of object oriented and traditional, procedural programming was used to achieve the functionalities needed.

4.1 External data structures and dependencies

Some open source third party tools and functions were used, customized and adapted in the toolbox. Some of these external functions were used as an inspiration, some heavily customized and some were used as is. The functions are integrated in the toolbox, so there are no external dependencies that could affect the functionality. The third-party functions used in the toolbox are listed in Table 5.

Table 5. *Usage of external functions*

Original function / used in toolbox function	**Source**
edfread [3]	From MathWorks File Excange, used as an inspiration and modified to suit needs
xml2struct [4]	From MathWorks File Excange, used as is
randmio / randomgraph [5]	From brain connectivity toolbox, customized/fixed for own needs
degrees_und / avgDegree [5] degrees_dir / avgDegree [5] clustering_coef / avgClusterCoeff [5]	From brain connectivity toolbox, customized for own needs and used as an inspiration

The only external data format the toolbox uses is the EDF format that is considered as de facto standard for polygraphic physiological data (Table 6). The EEG data read into the toolbox must obey the EDF format and strictly follow the specification of Table 6.

[3] https://www.mathworks.com/matlabcentral/fileexchange/31900-edfread
[4] https://www.mathworks.com/matlabcentral/fileexchange/28518-xml2struct
[5] https://sites.google.com/site/bctnet/Home/functions

Table 6. *European Data Format specification. "ns" stands for the number of channels present in the recording* (Kemp et al. 1992).

HEADER RECORD
8 ascii : version of this data format (0)
80 ascii : local patient identification
80 ascii : local recording identification
8 ascii : startdate of recording (dd.mm.yy)
8 ascii : starttime of recording (hh.mm.ss)
8 ascii : number of bytes in header record
44 ascii : reserved
8 ascii : number of data records (-1 if unknown)
8 ascii : duration of a data record, in seconds
4 ascii : number of signals (ns) in data record
ns * 16 ascii : ns * label (e.g. EEG Fpz-Cz or Body temp
ns * 80 ascii : ns * transducer type (e.g. AgAgCl electrode)
ns * 8 ascii : ns * physical dimension (e.g. uV or degreeC)
ns * 8 ascii : ns * physical minimum (e.g. -500 or 34)
ns * 8 ascii : ns * physical maximum (e.g. 500 or 40)
ns * 8 ascii : ns * digital minimum (e.g. -2048)
ns * 8 ascii : ns * digital maximum (e.g. 2047)
ns * 80 ascii : ns * prefiltering (e.g. HP:0.1Hz LP:75Hz)
ns * 8 ascii : ns * nr of samples in each data record
ns * 32 ascii : ns * reserved

DATA RECORD
nr of samples[1] * integer : first signal in the data record
nr of samples[2] * integer : second signal
..
..
nr of samples[ns] * integer : last signal

4.2 Toolbox

The modules of the toolbox are formed of groups of classes that together provide the functionality for each module.

A main program was also implemented, so that the whole process can be run without intervention. The main program can be considered as a part of the toolbox that integrates the independent modules together and acts as an automation engine. The following sections describe the structure and methodology of the toolbox.

4.2.1 General structure of the toolbox

At high level, the toolbox consists of three main parts (Figure 21): Data extraction and pre-processing, Calculation of the connectivity matrix and Calculation of network measures. These are described in more detail in the following sections. Generally, each part consists of several classes and external helper functions.

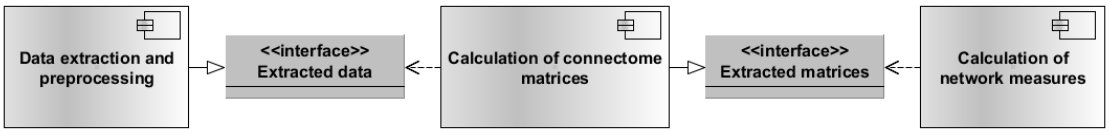

Figure 21. *A high level structure of the toolbox.*

The internal functionality of the modules is illustrated in Figure 22. The top lane represents the data extraction and preprocessing and the bottom lane describes the top-level functionality of the calculation process.

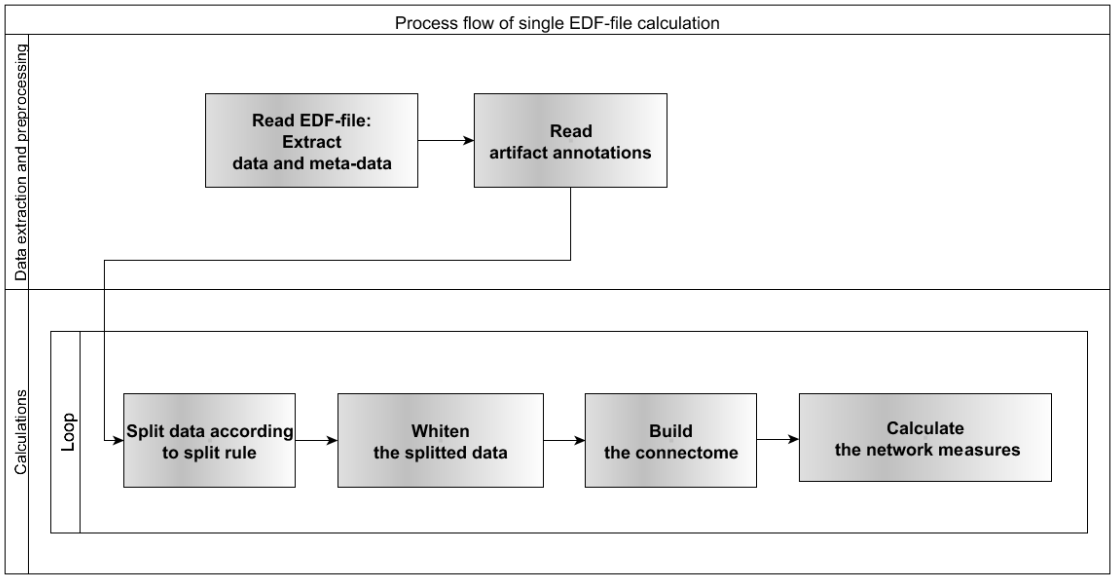

Figure 22. *A rough process chart of processing a single EDF file.*

At a more technical level, an informal class dependency diagram of the toolbox is presented in Figure 23. The diagram contains all the methods and public attributes of each class. External (off-class) helper functions are not included in this diagram. The toolbox contains both self-made and third-party helper functions.

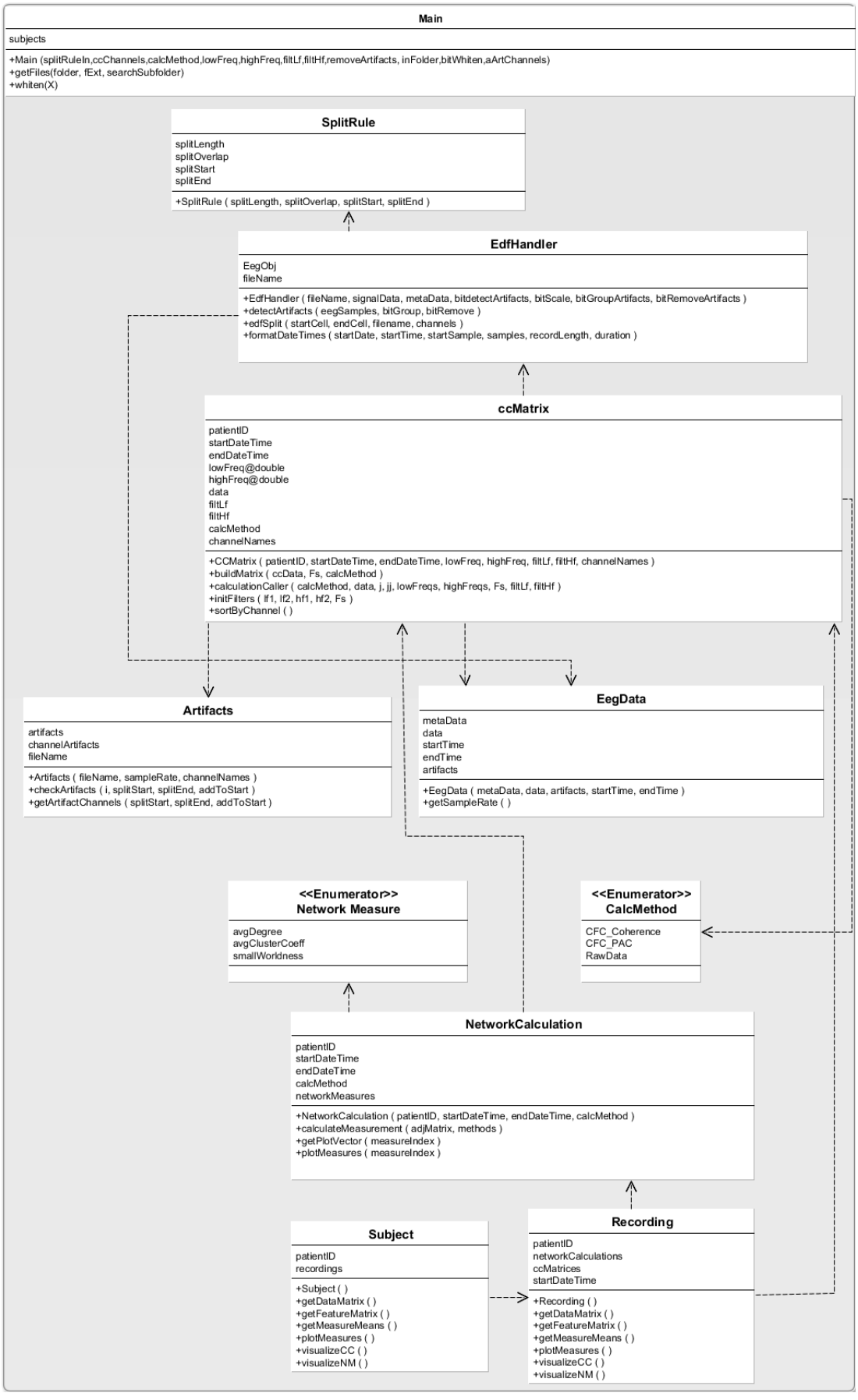

Figure 23. *Class dependency diagram.*

4.2.2 Data extraction and pre-processing

Data extraction part of the toolbox is responsible for reading the given EDF files, forming objects of type *EegData* from the data read and splitting the data into smaller chunks for calculation. The structure of the *EegData* object is shown in Code 1 and Figure 24. It contains a struct type variable *metaData* that is derived from the structure of the EDF header and transformed into a form of a struct for easier handling. The data matrix contains the data samples of the recording read into an object derived from this class. The recording start and end times are stored in separate variables.

```
classdef EegData < handle
    properties
        metaData@struct;
        data@single;
        startTime@datetime;
        endTime@datetime;
        artifacts@single
    end

    methods
        function self=EegData(metaData, data, artifacts, startTime, endTime)
        end
        function sampleRate = getSampleRate(self)
        end
    end
end
```

Code 1. *On-code class defintion of the EegData class.*

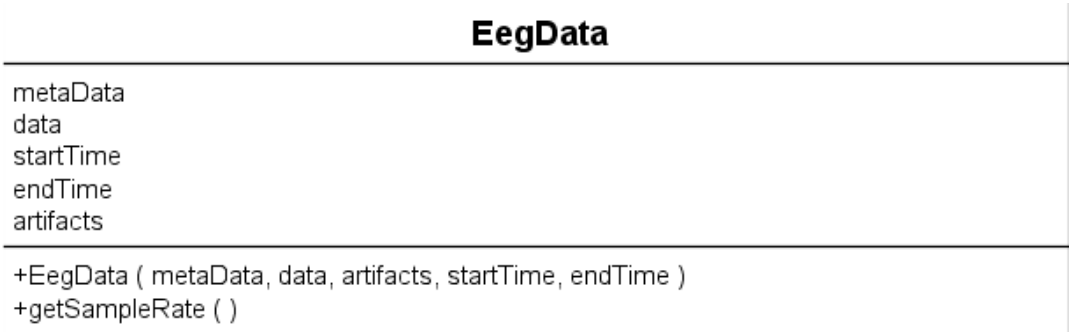

Figure 24. *The EegData class.*

The pre-processing part of the toolbox is somewhat shattered throughout the toolbox. Pre-processing includes artifact detection and removal, data whitening and normalization. The toolbox contains two different options for artifact detection and removal.

Reading the EDF files

The *EdfHandler* class of the toolbox is responsible for reading the data from the EDF files. The EDF format consists of a header record and a data record. The toolbox converts this format into a class format of its own. The information of a single recording is read

into a toolbox's internal object of a type *EegData*. The *EegData* derived object stores the information of the header record and the data record into separate matrices. These are both properties of an object derived from the *EegData* class along with some basic information variables. These matrices are called *metaData* and *data*.

As the EDF format is a fixed length file format, it is read using the *fread* function of Matlab. The function takes the length of data to be read as a parameter and moves the pointer to the location after the previously read value. This allows an easy way of reading through a fixed length file.

Automated artifact detection and removal

Automated artifact detection was implemented as a separate function in the toolbox's read functionality. The usage of the automated detection and removal of artifacts is separately parametrized and by default those are not used. Automated artifact detection is implemented as a simple function that compares the power of a signal in a signal segment to given thresholds. If the power is too high or too low (i.e., the signal is close to a flat line) the corresponding samples are marked as artefacts in a separate matrix. The matrix of artifact positions can then be taken into account when calculating the network measures or presenting the connectome values and handled according to the application.

Two other threshold values that can be set dictate the number of artefactual channels needed to cause a rejection of the whole window and the number of artefactual samples needed to cause the rejection of the whole channel. The function returns 3 matrices: artifacts, artefactual channels and the EEG samples. EEG samples are returned because, if the artifact removal is set active, the removal process is executed inside the function.

Annotation file based artifact removal

A more flexible and accurate way of handling the artefactual and/or other unwanted samples is the annotation file based artifact removal method. The basic principle of the method requires an expert to visually examine the EEG data and to create annotation files of the artefactual samples in each recording. Using these annotation files, the toolbox's read functionality looks for annotation files sharing the name with the input file. Instead of an edf extension, it looks for a file with xml extension from the input folder.

Depending on the annotation, the artifacts are dealt in different ways. The annotation file can include information about artifacts in a single channel, in multiple channels or, alternatively, all channels can be set as artefactual in a given timeframe. The duration of the artefactual segment can be set by the duration element of the XML file or the annotation's description element may contain reserved strings "[Start]" and "[End]", which are used as the beginning and the end of the artefactual timeframe. The reason for two different approaches is the way artifacts are visually annotated using the EDFbrowser.

The only annotation file format currently supported is the XML format of the EDFbrowser application. XML files of the accepted format can also be generated elsewhere. The format must follow the schema of Code 2. The schema was created based on EDFbrowser's XML output.

```
<xs:schema xmlns:xs="http://www.w3.org/2001/XMLSchema">
  <xs:element name="annotationlist">
    <xs:complexType>
      <xs:sequence>
        <xs:element type="xs:dateTime" name="recording_start_time"/>
        <xs:element name="annotation" maxOccurs="unbounded" minOccurs="0">
          <xs:complexType>
            <xs:sequence>
              <xs:element type="xs:dateTime" name="onset"/>
              <xs:element type="xs:string" name="duration"/>
              <xs:element type="xs:string" name="description"/>
            </xs:sequence>
          </xs:complexType>
        </xs:element>
      </xs:sequence>
    </xs:complexType>
  </xs:element>
</xs:schema>
```

Code 2. *The XSD Schema of the XML annotation file.*

Whitening

By default, prior to calculation, the data matrix is transformed using the whitening transformation. This is done in order to decorrelate and normalize the data. By default, the whitening transformation is executed, but it can be bypassed using correct parametrization.

4.2.3 Calculation of connectivity matrices

This part of the toolbox calculates connectivity matrices of the given data. The data can be provided by the data extraction module or it can be imported externally. Either way, the data must be of type *EegData* introduced in the previous section.

The process starts by creating an object of type *CCMatrix*, which is the class that is mainly responsible for everything related directly to the connectivity matrix. The class definition given in Code 3 and Figure 25 shows the public properties and methods of the class.

```
classdef CCMatrix < handle
    properties
        patientID
        startDateTime
        endDateTime
        lowFreq@double
        highFreq@double
        data@single
        filtLf@double
```

```
        filtHf@double;
        calcMethod@CalcMethod
        channelNames
    end
    properties (Constant)
        defaultLowFreq=[1,3];
        defaultHighFreq=[8,12];
    end
    methods
        function this=CCMatrix(patien-
tID,startDateTime,endDateTime,lowFreq,highFreq,filtLf,filtHf,channelNames)
        function self=buildMatrix(self,ccData,Fs,calcMethod)
function self=sortByChannel(self)
        function calcMeasure = calculationCaller(self,calc-
Method,data,j,jj,lowFreqs,highFreqs,Fs,filtLf,filtHf
    methods (Static)
        function [filtLf,filtHf]= initFilters(lf1,lf2,hf1,hf2,Fs)

    end
end
```

Code 3. *The on-code class definition of the CCMatrix class.*

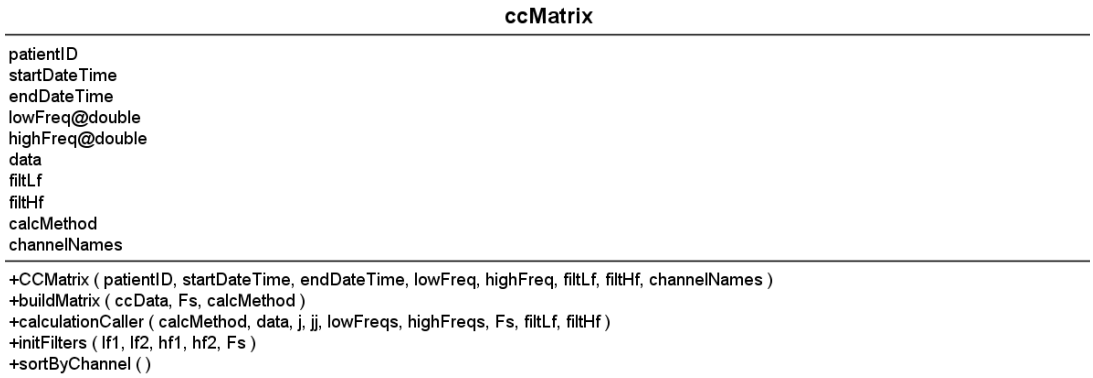

Figure 25. *The CCMatrix class.*

After calling the constructor to create a new object, the *buildMatrix* function of the object can be called with the necessary parameters. This function actually builds the matrix based on the given data and parameters. The data passed to the build function is just a numerical data matrix, which in this case contains a small preprocessed fragment of the whole EEG dataset. The data could as well be from any other source, so this calculation can be used in a quite versatile manner.

The actual calculation is also implemented modularly, so that anyone can add new calculation methods easily. This was achieved using a technique of assigning functions and variables dynamically based on the chosen calculation method. The data being processed is looped through in two nested loops, so that the synchronization level of every channel with every other channel is obtained. Inside the inner loop, a *calculationCaller* function of the object is called. The caller function creates a function handle and calls a function the name of which is given as a value of the parameter *calcMethod*. Due to the procedure,

every function implemented to calculate the connectivity matrix must have the same input parameters. A simplified version of the code is presented in Code 4 and Code 5.

```
parfor j=1:intChannels
      for jj=1:intChannels
            k=jj;

            ccMatrix(j,jj)= self.calculationCaller(calcMethod,data,j,jj…);
```

Code 4. *A code block of calling the caller function in a channel loop.*

```
function calcMeasure = calculationCaller(self,calcMethod,data,j,jj,…)
      if sum(isnan(data(j,:)))>0 || sum(isnan(data(jj,:)))>0
            calcMeasure=NaN;
      else
            funcHandle=str2func(char(calcMethod));
            calcMeasure =  funcHandle(data,j,jj,…);
      end
end
```

Code 5. *A code block of a caller function calling the actual function..*

Two calculation methods were implemented at this stage. These are coherence and PAC/PLV. The actual functions used for calculation are physically stored separately from the class. They are located in a separate *calculationMethods* folder, the path of which is added to the runtime environment using the helper function *addPaths*. The *addPaths* function is used in the *Main* program to add all the needed folders to the path of the Matlab environment. To keep things organized, each calculation function implemented must be introduced in an enumeration class called *CalcMethod*. The parametrization must also refer to the calculation method using these class members as static references. As an example, a default calculation method is set in the *Main* program as indicated in Code 6.

```
if nargin<3 || isempty(calcMethod)
    % Set default calculation method, if not selected
    calcMethod=CalcMethod.CFC_PAC;
end
```

Code 6. *Setting a calculation method variable.*

The theory behind the calculation methods has been introduced in chapter 3, but the implementation has not yet been discussed. The calculation method gets the following parameters, which are or are not used depending on the method:

- data — contains the data segment (matrix) to be processed
- j, jj — a channel to be used in the calculation
- lowFreqs — the cutoff frequency of the highpass filter
- highFreqs — the cutoff frequency of the lowpass filter
- Fs — sampling rate
- filtLf — the coefficients of the lowpass filter (optional)

- filtHf the coefficients of the highpass filter (optional).

The calculation of magnitude squared coherence is performed as follows. Data, sample rate and frequency boundaries are passed as parameters to the Matlab's *mscohere* function, which returns the result. To make the coherence calculation procedure faster, only the other half (upper or lower triangle) of the connectome matrix is processed as coherence has no directionality.

On the contrary, there is no inbuilt function to calculate the PAC/PLV in Matlab, so the calculation of this measure was implemented as a part of the toolbox. Code 7 shows the implementation which can be reflected to the theoretical description of the PAC/PLV measure presented in chapter 3.

```
function plvMean= CFC_PAC(data,j,jj,lowFreqs,highFreqs,Fs,filtLf,filtHf)

lf1=lowFreqs(1);
lf2=lowFreqs(2);
hf1=highFreqs(1);
hf2=highFreqs(2);

%Data is stored as single, but filtfilt needs double
data1=double(data(j,:));
data2=double(data(jj,:));

%If the filters are not given, create filters with given frequencies.
if isempty(filtLf) || isempty(filtHf)
    [filtLf,filtHf]=CCMatrix.initFilters(lf1,lf2,hf1,hf2);
end

%Get the low frequency part of data1
data1Lf = filtfilt(filtLf, 1, data1);

%Get the phase of the low frequency part
data1Phase = phase(hilbert(data1Lf));

%Get the high frequency of data2
data2Hf = filtfilt(filtHf, 1, data2);

%Get the amplitude envelope
data2Env = abs(hilbert(data2Hf));

%Get the low frequency of envelope
data2EnvLf = filtfilt(filtLf, 1, data2Env);

%Get phase of the lf part of hf
data2EnvPhase = phase(hilbert(data2EnvLf));

%Calculate PLV
plvMean=abs(mean(exp(1i.*(data1Phase - data2EnvPhase))));

end
```

Code 7. *The calculation function of PAC/PLV.*

After single iteration of Code 7, a value corresponding to the modulation of the amplitude in a predefined frequency band of channel *jj* by the phase of slow oscillations in channel *j* for the particular time window is obtained. In the *buildMatrix* function of the *CCMatrix* object the channels are all looped through in nested loops, so that each pair of channels will have two values in the matrix. For example, considering channels Fp1 and Fp2, there will be one value for Fp1→Fp2 and another value for, Fp2→Fp1. The first of each pair is the modulating channel of the PAC/PLV calculation.

After the initial procedures, a single *CCMatrix* object contains information and results of calculation regarding the data that was passed to it. In the *Main* program of the toolbox, the matrices are written to an object array that includes all the matrices of a single recording and are stored in an object derived from the class *Recording*. The object array formed from the recordings is a property of an object derived from the *Subject* class. In this way the structure leads to a *subject* object that contains *recording* arrays, which contain the actual connectivity matrices as indicated in Figure 26. The structures of the *Subject* and *Recording* classes are shown in Figure 27.

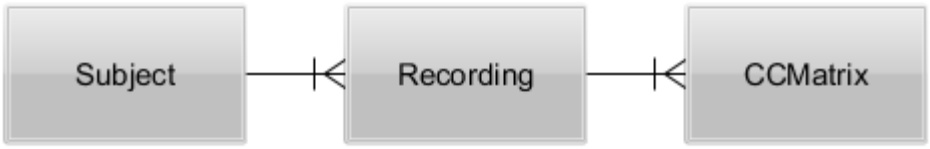

Figure 26. *Dependence diagram of Subject, Recording and CCMatrix classes.*

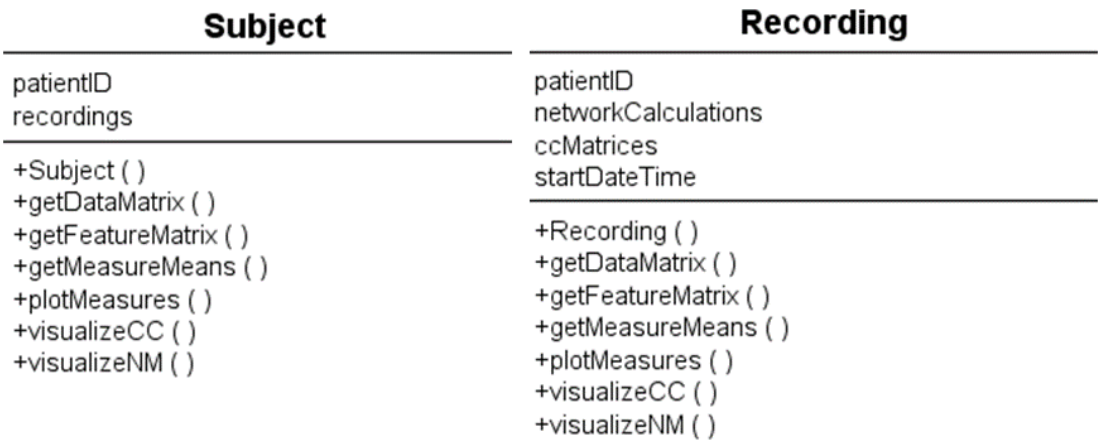

Figure 27. *Class diagrams of Subject and Recording classes.*

4.2.4 Network measures

The network measures part of the toolbox calculates certain measures from the connectivity matrices. As all parts of the toolbox, this part can also be used either independently

or with other modules of the toolbox. The class responsible for everything related to network measures and their calculation is the *NetworkCalculation* class (Code 8 and Figure 28). The class contains meta-information about the recording and the actual calculated data that are stored in a struct type variable *networkMeasures*. Besides the constructor, the most important public method of the class is the *calculateMeasurement* function, which triggers the calculation procedure.

```
classdef NetworkCalculation<handle
    properties
        patientID;              % Identificator of patient
        startDateTime;          % Correct date and time of start of this rec
        endDateTime;            % Correct date and time of end of this rec
        calcMethod@CalcMethod   % The method used for matrix calculation
        networkMeasures@struct; % Struct vector including name and value
    end
    methods
        function this=NetworkCalculation(patientID,startDateTime,endDate
        function self=calculateMeasurement(self,adjMatrix,methods)
        function self=plotMeasures(self, measureIndex)
        function [plotVector,title]=getPlotVector(self, measureIndex)
    end

end
```

Code 8. *Class definiton of the NetworkCalculation class.*

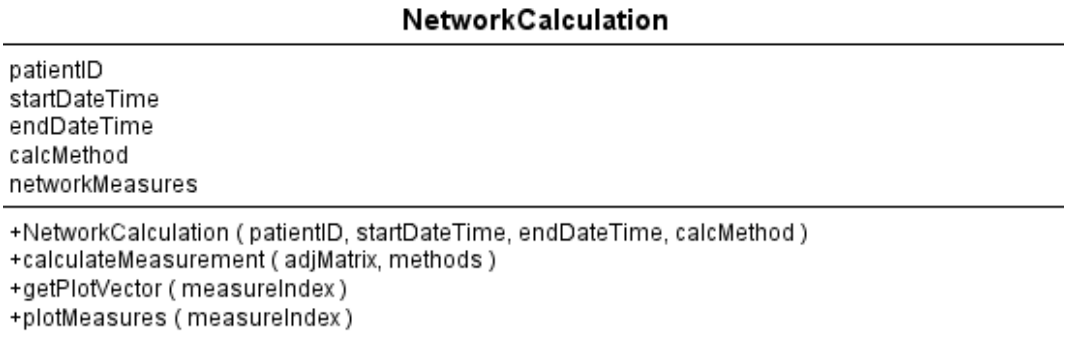

Figure 28. *Class diagram of the NetworkCalculation class.*

The calculation of network measures is also implemented modularly, so that measurements can be easily added at a later stage. This is achieved using a similar technique as in connectivity matrix calculation. The *calculateMeasurement* function takes in the connectivity matrix and the network measurements to be calculated as arguments and writes the calculated values to the *networkMeasures* variable of the current object using self-reference (Code 9). If the measures are not provided in the methods variable, all network measures that are defined in the *NetworkMeasure* enumeration class are calculated. The *NetworkMeasure* enumeration is similar to the *CalculationMethods* and differs only by its content. It lists and defines the possible network calculation methods.

```
function self=calculateMeasurement(self,adjMatrix,methods)
```

```
function self=calculateMeasurement(self,adjMatrix,methods)
      if isempty(methods)
        %If no methods given, add all possible measures to “methods”
        tmpNM=enumeration('NetworkMeasure');
        for i=1:size(tmpNM)
            methods=[methods;tmpNM(i)];
        end
      end
      %Calculate each measure given by “methods”.
      for i=1:size(methods)
        %Call the function called methods(i)
        funcHandle=str2func(char(methods(i)));
        self.networkMeasures(i).method =  methods(i);
        %Remove NaN-valued rows/cols
        adjMatrix(~any(~isnan(adjMatrix), 2),:)=[];
        adjMatrix(:,~any(~isnan(adjMatrix), 1))=[];

        self.networkMeasures(i).value=funcHandle(adjMatrix,self.calcMethod);
      end
end
```

Code 9. *The calculateMeasurement function.*

As with the connectivity matrix calculation methods, the functions for the network measure calculation also reside in a separate folder named *networkMeasures*. At this stage three calculation methods were implemented. These are Degree, Clustering coefficient and Smallworldness.

Using the *Main* program of the toolbox, the network measures are stored in an object array as a property of the *recording* object. Structurally they could have as well been a child object of the *CCMatrix* class, as they are directly calculated from the matrices. Figure 29 shows the dependency diagram after the addition of the *NetworkMeasure* class. The arrow from *NetworkMeasure* to *CCMatrix* refers to the relationship between the two classes as the *NetworkMeasure* class uses the *CCMatrix* class content and would not exist without it.

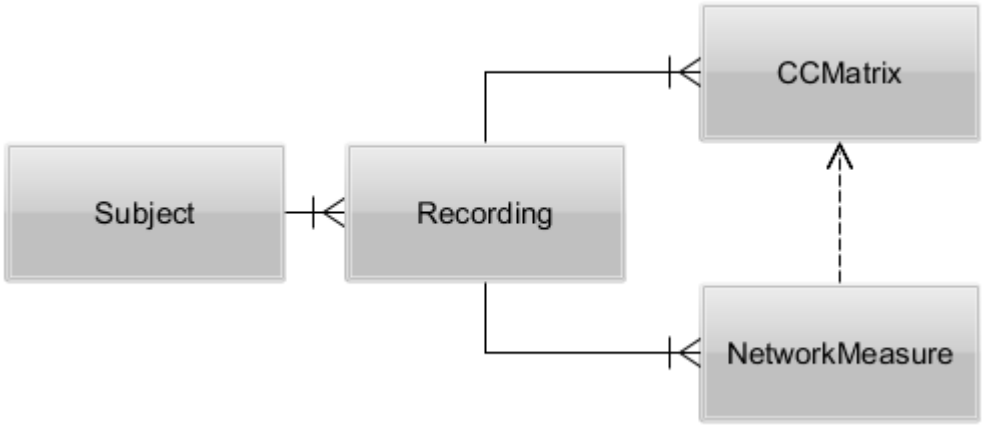

Figure 29. *Dependence diagram including the NetworkMeasure class.*

5. NETWORK ANALYSIS OF EEG IN TBI PATIENTS IN THE ICU

While building the toolbox, a structure of a real-life dataset was used as the basis of requirement. Part of this dataset was used to test the toolbox and to provide preliminary means for the analysis of the measures extracted from the data using the toolbox. The dataset and the calculation principles used as the basis of the analysis are presented in this chapter.

5.1 Data and patients

The dataset used in this thesis to test and develop the network analysis toolbox was provided and recorded by the ICU unit of Turku University Hospital. In total 30 patients were included in the study. The lengths and numbers of the recordings varied per patient as did the number of EEG channels recorded.

In the course of this thesis, 6 patients were selected based on the outcome of their condition, number of electrodes per recording and the length and number of the recordings. Equal number of patients were selected from both groups, those with positive and those with negative outcome of the treatment. All the patients studied here had the same EEG channels recorded, which made the comparison more straightforward. As the artifact detection/annotation was done manually and the annotation process was time consuming, it was agreed to preselect smaller number of patients to be used in the analysis.

As usual with EEG data, the selected recordings also included artifacts, which had to be dealt with. A simple artifact detection tool was built into the toolbox, but to get more consistent and reliable results, the artifact detection was done visually by examining the recordings and creating annotation files of the artifacts. These annotation files were then handled in the data reading phase of the toolbox. Data segments containing more than 2 artefactual channels were discarded completely and otherwise the corrupted channels were omitted during the connectome calculation. Prior to connectome calculation, each data segment was normalized using the whitening transformation.

5.2 Calculation of connectivity matrices

Both of the calculation methods (PAC/PLV and coherence) built into the toolbox were used to calculate connectivity matrices. Connectivity matrices based on coherence were calculated for frequency bands 8-13 and 13-35 Hz. The PAC/PLV connectivity matrices were calculated for modulated frequencies of 8-13 Hz and 13-35 Hz while the modulating frequency range was 0-2 Hz. The lower frequency range (low-delta) was chosen based

on visual inspection of the recordings and because of a recent discovery of the role of slow oscillations (< 1 Hz) in the assessment of brain dysfunction after brain injury (Kortelainen et al. 2017).

Channels included in this test study were Fp1, Fp2, F7, F3, Fz, F4, F8, T3, C3, Cz, C4, T4, T5, P3, Pz, P4, T6, O1 and O2 as seen from Figure 30. The channels are sorted to the connectivity matrices based on the 10-20 system positioning starting from the top-left (Fp1) and proceeding from left to right, top to bottom. Figure 30 shows two connectivity matrices composed of the PAC/PLV values of two separate time windows of the same recording. There are in total 19 channels indicated in the figure. Colder colors indicate smaller values and warmer colors higher values of phase locking between channels as indicated by the color bars of Figure 30. Connectivity matrix is an adjacency matrix, so each channel is included as a row and as a column and the diagonal represents the self-modulation between the frequencies chosen, in this case 0-2 Hz and 8-13 Hz. Two coherence based connectivity matrices of 1-30 Hz frequency band are presented in Figure 31. Matrices are from the same recording 10 minutes apart. Due to the nature of coherence, diagonal of the matrix is always fully coherent consisting of ones as values. In order to remove the diagonal dominance, the diagonal values of the matrix were set to zero. The undirectedness of the coherence based matrix can be seen by examining the values in a certain row and column and then vice versa. For example, the value in the second column of the first row is the same as the value in the first column of the second row.

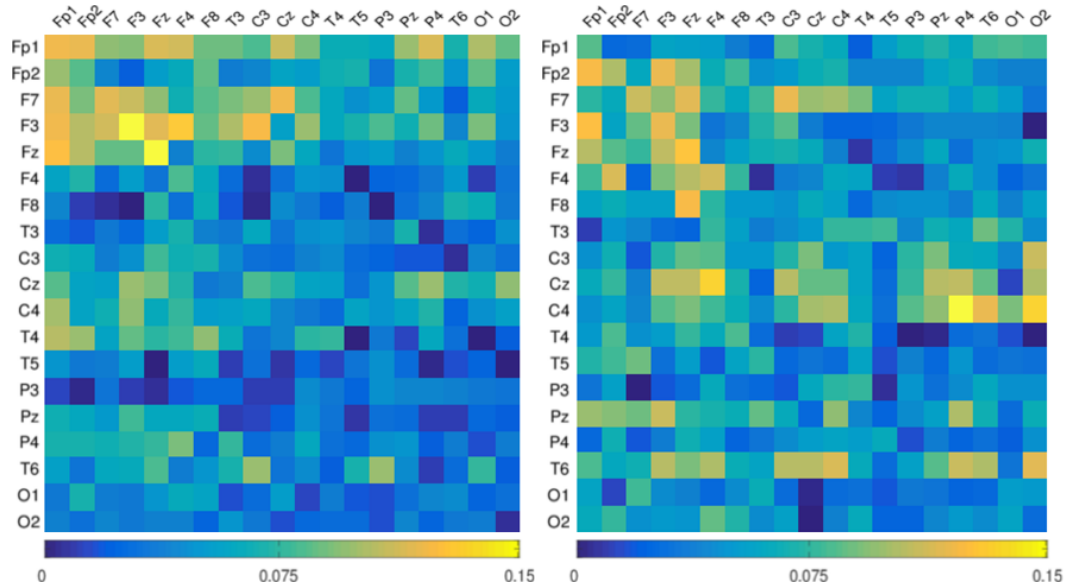

Figure 30. *Two examples of PAC/PLV connectivity matrices from the same recording 10 minutes apart. Frequency ranges used were 0-2 Hz (modulating) and 8-13 Hz (modulated).*

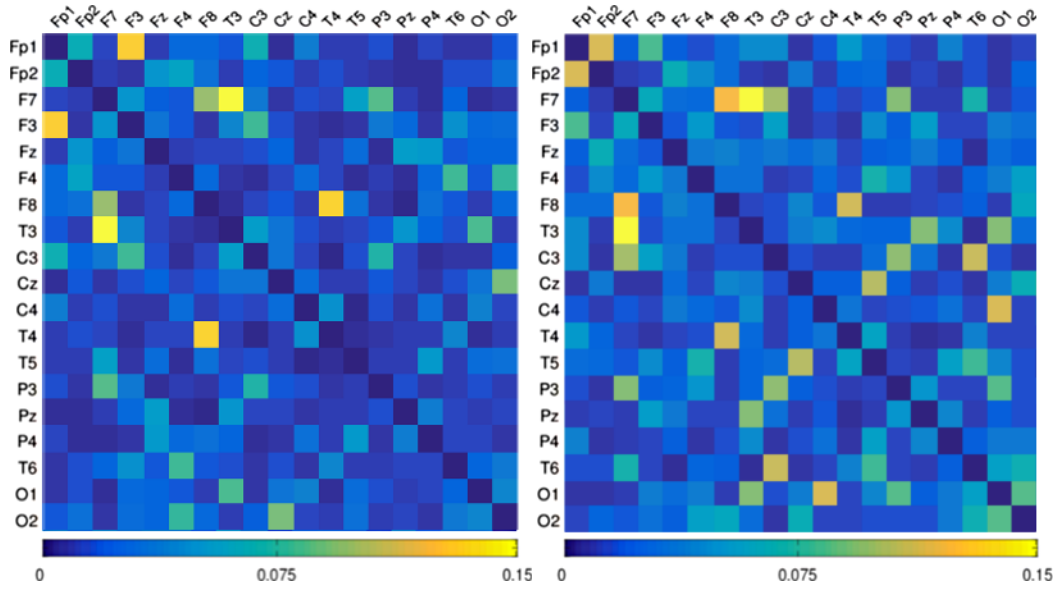

Figure 31. *Two examples of coherence based connectivity matrices from the same recording 10 minutes apart. Frequency range used was 1-30 Hz.*

5.3 Statistical analysis

For statistical comparison, the patients were divided into 2 groups based on the outcome of the treatment. Sample sizes of 4910 for the positive outcome (pos-group) and 4103 for the negative outcome (neg-group) were acquired from the dataset. The comparison was performed using the Mann-Whitney U-test, where the null hypothesis H_0 is that the two groups come from the same population. The test is carried out by comparing each data sample of the positive outcome group to each data sample of the negative outcome group and if the null hypothesis holds, the samples of the positive outcome group have equal probability of being greater or smaller than the samples in negative outcome group:

$$H_0: P(x_i > y_j) = \frac{1}{2}$$
$$H_1: P(x_i > y_j) \neq \frac{1}{2}.$$

The value of the U-statistic, obtained as the result of the test, represents the proportion of comparisons where y is smaller than x. The value was directly used as the predictor of patient's outcome. In comparison, the U-value is equal to the Area Under Curve (AUC) statistic of the Receiver Operating Characteristic (ROC).

5.4 Results

A matrix of U-values based on the PAC/PLV of 0-2 Hz band modulating 13-35 Hz frequency band is presented in Figure 32. Each cell of the matrix corresponds to the U-value

between the pos- and neg-groups. The values are represented using color coding expressed by the color bar below the matrix. Colder colors indicating lower values (neg-group dominance) and warmer colors higher values (pos-group dominance) in the scale of 0.1 to 0.9. The average U-value for each row is shown at the right side of the matrix. For example, the average U-value for Fp2 is approximately 0.7 according to Figure 32.

As Figure 32 indicates, there is a lot of variation in group dominance depending on the modulating channel. A potentially important observation can be made that the frontal channels (Fp1-Fz) and channels C4 and T4 seem to modulate other channels in a consistently higher magnitude in case of the patients of the pos-group. Likewise, on average, C3, Cz, P4 and the O-channels (O1 and O2) seem to have U-values below 0.5, indicating higher values in patients of the neg-group. Similar results were also seen when the frequency range being modulated was 8-13Hz.

A similar matrix of U-values based on the coherence at the frequency range of 13-35 Hz is shown in Figure 33. The coherence matrix shows a lot more randomness when compared to the PAC/PLV matrix (Figure 32). The average coherence of certain channels seems to be higher in the pos-group, but this can mainly be explained with a few exceptionally high values biasing the average in favor of the pos-group. However, in total the pos-group's averaged coherence was higher in 76 % of the test cases when compared to the neg-group. In the lower frequency range (8-13 Hz), there was no such difference, U-value being 0.49.

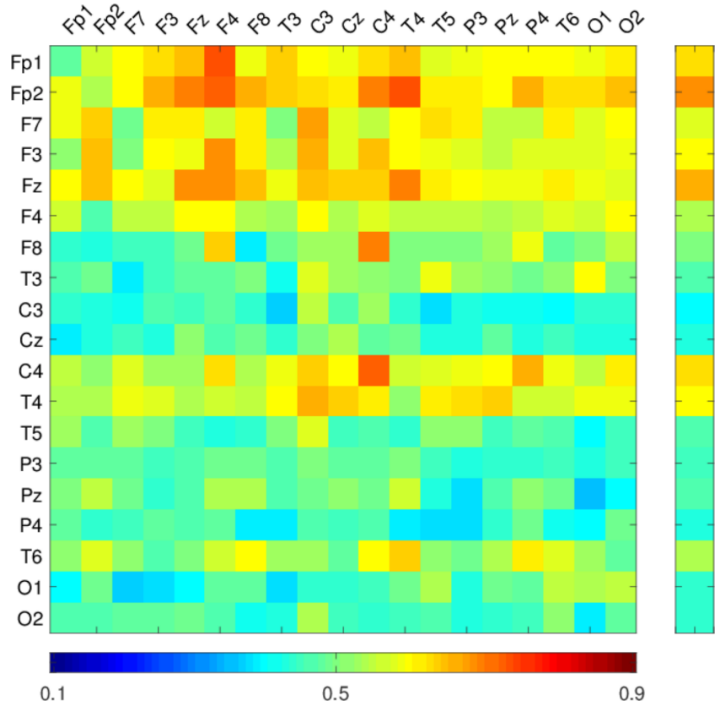

Figure 32. *Calculated U-statistic values for PAC/PLV (0-2Hz → 13-35 Hz) connectivity matrix and the average per channel* (Lipping et al. 2017)

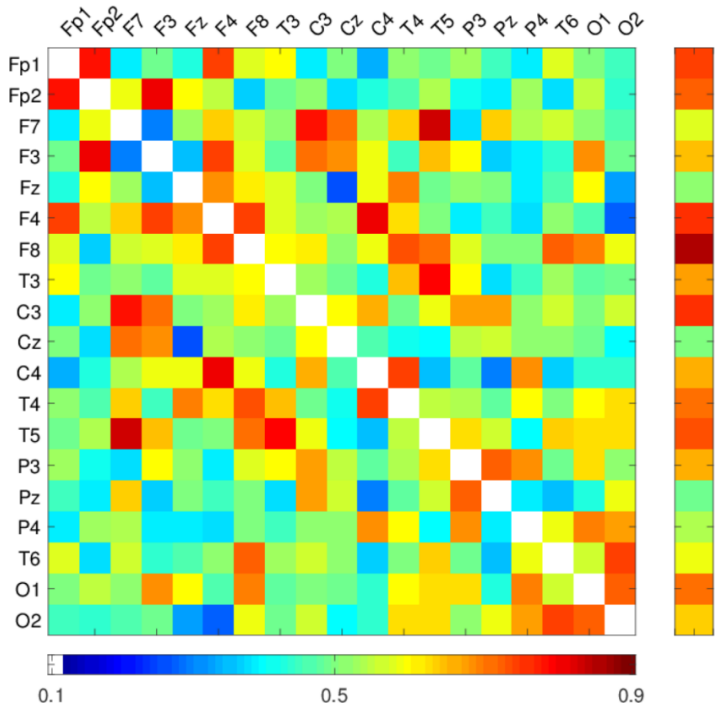

Figure 33. *Calculated U-statistic values for coherence (13-35 Hz) connectivity matrix and the average per channel* (Lipping et al. 2017).

6. CONCLUSIONS

The main scope of this thesis was to create a working prototype of a toolbox that could be used to analyze the network-like behavior of the human brain based on EEG recordings. During this thesis such toolbox was developed to a point that it can be used to calculate connectivity matrices and network measures from data stored in raw EDF files. The next phase of the toolbox development could be to implement a module or modules that take the network measures as input and analyze the variability and trends of these measures as the predictors of outcome. For example, the small-worldness of the brain varies significantly during the maturation of the brain and the same mechanism might also have a role in monitoring the TBI patients. One approach could be to cluster the network measures to separate classes and analyze the transitions between the states represented by the clusters.

The secondary objective of this thesis was to test the toolbox by analyzing a dataset of TBI patients. The analysis of the data from 6 patients suggests that the techniques used might have a correlation with the outcome of the patients and could be used for monitoring and outcome prediction in TBI patients. Currently the number of patients is too small for the results to have real clinical value, however, in the next phase of the study the whole data set will be analyzed and a broader set of methods and method parameters will be tested. Further analysis is also needed to specify more accurately the frequency bands yielding best predictors. Other connectivity measures should also be implemented into the toolbox and used to analyze the connectivity.

REFERENCES

Akin, M., 2002. Comparison of wavelet transform and FFT methods in the analysis of EEG signals. *Journal of Medical Systems*, 26(3), pp.241–247.

Andersen, P. & Andersson, S.A., 1968. Physiological Basis of the Alpha Rhythm, *Appleton-Century-Crofts*.

Azevedo, F.A.C. et al., 2009. Equal numbers of neuronal and nonneuronal cells make the human brain an isometrically scaled-up primate brain. *The Journal of Comparative Neurology*, 513(5), pp.532–541.

Barwick, D.D., 1971. Hans Berger on the electroencephalogram of man. The fourteen original reports on the human electroencephalogram. *Journal of the Neurological Sciences*, 13(4), p.507.

Berger, H., 1929. Über das Elektrenkephalogramm des Menschen. *Archiv für Psychiatrie und Nervenkrankheiten*, 87(1), pp.527–570.

Boersma, M. et al., 2011. Network analysis of resting state EEG in the developing young brain: Structure comes with maturation. *Human Brain Mapping*, 32(3), pp.413–425.

Bruhn, J. et al., 2003. Correlation of approximate entropy, bispectral index, and spectral edge frequency 95 (SEF95) with clinical signs of "anesthetic depth" during coadministration of propofol and remifentanil. *Anesthesiology*, 98(3), pp.621–7.

Calcagno, S., La Foresta, F. & Versac, M., 2014. Independent Component Analysis and Discrete Wavelet Transform for Artifact Removal in Biomedical Signal Processing. *American Journal of Applied Sciences*, 11(1), pp.57–68.

Centorrino, F. et al., 2002. EEG Abnormalities During Treatment With Typical and Atypical Antipsychotics. *American Journal of Psychiatry*, 159(1), pp.109–115.

Chien Yong, G., Maan, N. & Ahmad, T., 2013. EEG Signal of Epiliptic Patient by Fast Fourier and Wavelet Transforms. *Jurnal Teknologi*, 61(1), pp.13-20.

Claassen, J. et al., 2004. Detection of electrographic seizures with continuous EEG monitoring in critically ill patients. *Neurology*, 62(10), pp.1743–8.

Davey, B.L.K. et al., 1989. Expert system approach to detection of epileptiform activity in the EEG. *Medical & Biological Engineering & Computing*, 27(4), pp.365–370.

Dimitriadis, S.I. et al., 2015. Cognitive Workload Assessment Based on the Tensorial Treatment of EEG Estimates of Cross-Frequency Phase Interactions. *Annals of Biomedical Engineering*, 43(4), pp.977–989.

Empson, J., 1986. Human brainwaves, *The Macmillan Press Ltd.*

Fornito, A., Zalesky, A. & Bullmore, E.T., 2016. Fundamentals of brain network analysis, *Academic Press.*

Garces Correa, M.A. & Laciar, E., 2011. Noise Removal from EEG Signals in Polisomnographic Records Applying Adaptive Filters in Cascade, Adaptive Filtering Applications. *InTech*.

Haas, L.F., 2003. Hans Berger (1873-1941), Richard Caton (1842-1926), and electroencephalography. *Journal of neurology, neurosurgery, and psychiatry*, 74(1), p.9.

Herman, S.T. et al., 2015. Consensus Statement on Continuous EEG in Critically Ill Adults and Children, Part II : Personnel , Technical Specifications, and Clinical Practice. *Journal of clinical neurophysiology*, 32(2), pp.96–108.

Hirsch, L.J. et al., 2013. American Clinical Neurophysiology Society's Standardized Critical Care EEG Terminology: 2012 version. *Journal of clinical neurophysiology*, 30(1), pp.1-27.

Hirsch, L.J., 2004. Continuous EEG monitoring in the intensive care unit: an overview. *Journal of clinical neurophysiology : official publication of the American Electroencephalographic Society*, 21(5), pp.332–40.

Humphries, M.D. & Gurney, K., 2008. Network ´Small-World-Ness´: A Quantitative Method for Determining Canonical Network Equivalence. *PLoS ONE*, 3(4).

Jennett, B. et al., 1981. Disability after severe head injury: observations on the use of the Glasgow Outcome Scale. *Journal of neurology, neurosurgery, and psychiatry*, 44(4), pp.285–93.

Jennett, B. & Bond, M., 1975. Assessment of outcome after severe brain damage. *Lancet (London, England)*, 1(7905), pp.480–4.

Jensen, O. & Colgin, L.L., 2007. Cross-frequency coupling between neuronal oscillations. *Trends in cognitive sciences*, 11(7), pp.267–9.

Jeong, J., 2004. EEG dynamics in patients with Alzheimer's disease. *Clinical Neurophysiology*, 115(7), pp.1490–1505.

Jordan, K.G., 1993. Continuous EEG and evoked potential monitoring in the neuroscience intensive care unit. *Journal of clinical neurophysiology : official publication of the American Electroencephalographic Society*, 10(4), pp.445–75.

Joudaki, A. et al., 2012. EEG-Based Functional Brain Networks: Does the Network Size Matter? P. A. Valdes-Sosa, ed. *PLoS ONE*, 7(4), p.9.

Kaplan, J.A., 2008. Essentials of cardiac anesthesia, *Saunders*.

Kemp, B. et al., 1992. A simple format for exchange of digitized polygraphic recordings. *Electroencephalography and clinical neurophysiology*, 82(5), pp.391–3.

Klass, D.W., 1995. The Continuing Challenge of Artefacts in the EEG. *The American Journal of EEG Technology*, 35, pp.239–269.

Klem, G.H. et al., 1999. The ten ± twenty electrode system of the International Federation.

Electroencephalography and clinical neurophysiology. Supplement, 52, pp. 3-6.

Kortelainen, J. et al., 2017. Pilot Study of Propofol-induced Slow Waves as a Pharmacologic Test for Brain Dysfunction after Brain Injury. *Anesthesiology*, 126(1), pp.94–103.

Lachaux, J. et al., 1999. Measuring Phase Synchrony in Brain Signals. *Human Brain Mapping*, 208, pp.194–208.

Lachaux, J.-P. et al., 2005. The many faces of the gamma band response to complex visual stimuli. *NeuroImage*, 25(2), pp.491–501.

Lipping, T. et al., 2017. Connectivity Analysis of Full Montage EEG in Traumatic Brain Injury Patients in the ICU. *Paper presented to Joint conference of European Medical and Biological Engineering Conference (EMBEC), Tampere, 11-15 June.*

Luce, D.R. & Perry, A.D., 1949. A method of matrix analysis of group structure. *Psychometrika*, 14(1), pp.95-116.

Mack, C.A., 2011. Analytic form for the power spectral density in one, two, and three dimensions. *Journal of Micro/Nanolithography, MEMS, and MOEMS*, 10(4).

Malmivuo, J. & Plonsey, R., 1995. Bioelectromagnetism: Principles and Applications of Bioelectric and Biomagnetic Fields, *Oxford University Press*.

Matsuura, M. et al., 1985. Age development and sex differences of various EEG elements in healthy children and adults — Quantification by a computerized wave form recognition method. *Electroencephalography and Clinical Neurophysiology*, 60(5), pp.394–406.

Milgram, S., 1967. The Small-World Problem. *Psychology Today*, 1(1), pp.61–67.

Millett, D., 2001. Hans Berger: From Psychic Energy to the EEG. *Perspectives in Biology and Medicine*, 44(4), pp.522–542.

Miltner, W.H.R. et al., 1999. Coherence of gamma-band EEG activity as a basis for associative learning. *Nature*, 397(6718), pp.434–436.

Muthukumaraswamy, S.D., 2013. High-frequency brain activity and muscle artifacts in MEG/EEG: a review and recommendations. *Frontiers in human neuroscience*, 7, p.138.

Newman, M.E.J., 2003. The structure and function of complex networks. *SIAM Review, 45, pp.167-256.*

Newman, M.E.J., 2010. Networks : an introduction, *Oxford University Press*.

Newman, M.E.J., Watts, D.J. & Strogatz, S.H., 2002. Random graph models of social networks. *Proceedings of the National Academy of Sciences of the United States of America*, 99(1), pp.2566–72.

Ney, J.P. et al., 2013. Continuous and routine EEG in intensive care: utilization and

outcomes, United States 2005-2009. *Neurology*, 81(23), pp.2002–8.

Nieuwenhuijs, D. et al., 2002. Bispectral Index Values and Spectral Edge Frequency at Different Stages of Physiologic Sleep. *Anesthesia & Analgesia*, 94(1), pp.125–129.

Olejniczak, P., 2006. Neurophysiologic Basis of EEG. *Journal of Clinical Neurophysiology*, 23(3), pp.186–189.

Opsahl, T. & Panzarasa, P., 2009. Clustering in weighted networks. *Social Networks*, 31(2), pp.155–163.

Penny, W.D. et al., 2008. Testing for nested oscillation. *Journal of Neuroscience Methods*, 174, pp.50–61.

Reches, A. et al., 2017. Preliminary investigation of Brain Network Activation (BNA) and its clinical utility in sport-related concussion. *Brain Injury*, 31(2), pp.237–246.

Rubinov, M. & Sporns, O., 2010. NeuroImage Complex network measures of brain connectivity : Uses and interpretations. *NeuroImage*, 52(3), pp.1059–1069.

Saramäki, J. et al., 2007. Generalizations of the clustering coefficient to weighted complex networks. *Physical Review E*, 75(2).

Schwilden, H., 1989. Use of the median EEG frequency and pharmacokinetics in determining depth of anaesthesia. *Baillière's Clinical Anaesthesiology*, 3(3), pp.603–621.

Si, Y. et al., 1998. An expert system for EEG monitoring in the pediatric intensive care unit. *Electroencephalography and Clinical Neurophysiology*, 106(6), pp.488–500.

Soffer, S.N. & Vázquez, A., 2005. Network clustering coefficient without degree-correlation biases. *Physical Review E*, 71(5).

Sporns, O., Tononi, G. & Kötter, R., 2005. The Human Connectome: A Structural Description of the Human Brain. *PLoS Computational Biology*, 1(4).

Szeto, H.H., 1990. Spectral Edge Frequency as a Simple Quantitative Measure of the Maturation of Electrocortical Activity. *Pediatric Research*, 27(3), pp.289–292.

Taelman, J., Van Huffel, S. & Spaepen, A., 2007. Wavelet-independent component analysis to remove electrocardiography contamination in surface electromyography. *Annual International Conference of the IEEE Engineering in Medicine and Biology - Proceedings*, pp.682–685.

Teasdale, G. et al., 2014. The Glasgow Coma Scale at 40 years: standing the test of time. *The Lancet. Neurology*, 13(8), pp.844–54.

Teasdale, G. & Jennett, B., 1974. Assessment of coma and impaired consciousness. A practical scale. *Lancet*, Jul 13(2), pp.81–4.

Teasdale, G.M. et al., 1998. Analyzing Outcome of Treatment of Severe Head Injury: A Review and Update on Advancing the Use of the Glasgow Outcome Scale. *Journal*

of Neurotrauma, 15(8), pp.587–597.

Teplan, M., 2002. Fundamentals of EEG Measurement. *Measurement Science Review*, 2(2), pp.1–11.

Tort, A.B.L. et al., 2010. Measuring Phase-Amplitude Coupling Between Neuronal Oscillations of Different Frequencies. *Journal of Neurophysiology*, *104(4)*, pp.1195–1210.

Trinka, E. & Leitinger, M., 2015. Which EEG patterns in coma are nonconvulsive status epilepticus? *Epilepsy & Behavior*, 49, pp.203–222.

Vecchio, F. et al., 2016. Cortical connectivity and lesion volumes correlation in acute stroke patients: A study via graph theory from EEG data. *Clinical Neurophysiology*, 127(3).

Vespa, P.M. et al., 1999. Increased incidence and impact of nonconvulsive and convulsive seizures after traumatic brain injury as detected by continuous electroencephalographic monitoring. *Journal of Neurosurgery*, 91(5), pp.750–760.

De Vico Fallani, F. et al., 2010. Cortical Network Analysis in Patients Affected by Schizophrenia. *Brain Topography*, 23(2), pp.214–220.

Vuckovic, A. et al., 2002. Automatic recognition of alertness and drowsiness from EEG by an artificial neural network. *Medical Engineering & Physics*, 24(5), pp.349–360.

Watts, D.J. & Strogatz, S.H., 1998. Collective dynamics of 'small-world' networks. *Nature*, 393(6684), pp.440–442.

Weir, J. et al., 2012. Does the extended Glasgow Outcome Scale add value to the conventional Glasgow Outcome Scale? *Journal of neurotrauma*, 29(1), pp.53–8.

Wen, D., Zhou, Y. & Li, X., 2015. A critical review: coupling and synchronization analysis methods of EEG signal with mild cognitive impairment. *Frontiers in aging neuroscience*, 7, p.54.

van Wijk, B.C.M., Stam, C.J. & Daffertshofer, A., 2010. Comparing brain networks of different size and connectivity density using graph theory. *PloS one*, 5(10).

Winkler, I., Haufe, S. & Tangermann, M., 2011. Automatic Classification of Artifactual ICA-Components for Artifact Removal in EEG Signals. *Behavioral and Brain Functions*, 7(1), p.30.

Witsch, J. et al., 2017. Electroencephalographic Periodic Discharges and Frequency-Dependent Brain Tissue Hypoxia in Acute Brain Injury. *JAMA Neurology*, *74(3), pp.301-309*.

Yamaguchi, C., 2003. Fourier and wavelet analyses of normal and epileptic electroencephalogram (EEG). In *First International IEEE/EMBS Conference on Neural Engineering, NER. Conference Proceedings.* IEEE, pp. 406–409.